Synthesis and Characterization of a Novel Vinyl-2,2′-bipyridine Monomer and Its Homopolymeric/Copolymeric Metal Complexes

Elefterios K. Pefkianakis, Nikolaos P. Tzanetos, and Joannis K. Kallitsis*

Department of Chemistry, University of Patras, 26500 Patras, Greece

Received March 31, 2008. Revised Manuscript Received July 8, 2008

Novel hybrid materials, based on polymeric ruthenium complexes, have been synthesized and characterized. The preparation of a new vinylic tris(bipyridine)ruthenium complex in high yields enabled the synthesis of soluble polymeric materials with high metal loading, using a controlled polymerization technique such as atom transfer radical polymerization. Moreover, combination of this monomeric complex with other monomers, known for their electron or hole transporting properties, led to soluble copolymers of various desired ruthenium loadings. Characterization of the synthesized polymers and copolymers was performed using NMR, SEC, and viscometry. The polymer−metal hybrid materials' optical properties were studied in detail through UV−vis and photoluminescence spectroscopies, showing the [$Ru^{II}(bpy)_3$] complexes' intense optoelectronic characteristics, also in combination with the optical properties of the oxadiazole or carbazole units in the copolymer case.

Introduction

The introduction of metal−ligand bonding into polymers brings novel and potentially useful physical and chemical properties to the final polymeric complexes.[1−5] These properties arise from the combination of both the metal ion (oxidoreductive, optoelectronic, catalytic) and the polymers' characteristics (processability, mechanical strength, thin film formation, etc.). The incorporation of metal binding sites into polymers can be performed either along the main chain[6−11] or as side group functionalities.[12−22] To enable metal complexation, bidentate and tridentate ligands such as 2,2′-bipyridine (bpy) and 2,2′:6′,2″-terpyridine (tpy) are mainly used, as well as some nitrogen-containing heterocycles,[1] through which the introduction of various transition-metal ions such as Fe(II), Cu(II), Os(II), Ir(II), and Ru(II) can be achieved.[1,2,5,6,8,22−28] Among these ions, ruthenium(II) is the most promising for the creation of polymeric metal complexes, since it allows the direct synthesis of both symmetric and nonsymmetric, stable systems.[22−31] Moreover, ruthenium complexes of bipyridine ligands are considered ideal for optoelectronics in comparison to terpyridine ligands, since they present fine absorption properties and higher luminescence and charge transport efficiency.[1,24,25]

In particular, tpy−Ru(II)−tpy complexes have been extensively used as main chain polymeric functionalities for

* To whom correspondence should be addressed. Phone: +30-2610-997121. Fax: +30-2610-997-122. E-mail: j.kallitsis@chemistry.upatras.gr.

(1) Schubert, U. S.; Eschbaumer, C. *Angew. Chem., Int. Ed.* **2002**, *41*, 2829.
(2) Whittell, G. R.; Manners, I. *Adv. Mater.* **2007**, *19*, 3439.
(3) Fustin, C. A.; Guillet, P.; Schubert, U. S.; Gohy, J. F. *Adv. Mater.* **2007**, *19*, 1665.
(4) Williams, K. A.; Boydston, A. J.; Bielawski, C. W. *Chem. Soc. Rev.* **2007**, *36*, 729.
(5) Abruña, H. D.; Denisevich, P.; Umaña, M.; Meyer, T. J.; Murray, R. W. *J. Am. Chem. Soc.* **1981**, *103*, 1.
(6) Heller, M.; Schubert, U. S. *Macromol. Rapid Commun.* **2001**, *22*, 1358.
(7) Guerrero-Sanchez, C.; Lohmeijer, B. G. G.; Meier, M. A. R.; Schubert, U. S. *Macromolecules* **2005**, *38*, 10388.
(8) Chiper, M.; Meier, M. A. R.; Wouters, D.; Hoeppener, S.; Fustin, C.-A.; Gohy, J.-F.; Schubert, U. S. *Macromolecules* **2008**, *41*, 2771.
(9) Knapp, R.; Schott, A.; Rehahn, M. *Macromolecules* **1996**, *29*, 478.
(10) Kelch, S.; Rehahn, M. *Macromolecules* **1997**, *30*, 6185.
(11) Kelch, S.; Rehahn, M. *Macromolecules* **1999**, *32*, 5818.
(12) Jones, W. E., Jr.; Baxter, S. M.; Strouse, G. F.; Meyer, T. J. *J. Am. Chem. Soc.* **1993**, *115*, 7363.
(13) Calzia, K. J.; Tew, G. N. *Macromolecules* **2002**, *35*, 6090.
(14) Aamer, K. A.; De Jeu, W. H.; Tew, G. N. *Macromolecules* **2008**, *41*, 2022.
(15) Serin, J. X.; Andronov, S. A.; Fréchet, J. M. J. *Macromolecules* **2002**, *35*, 5396.
(16) Chen, B.; Sleiman, H. F. *Macromolecules* **2004**, *37*, 5866.
(17) Heller, M.; Schubert, U. S. *Macromol. Rapid Commun.* **2002**, *23*, 411.
(18) Schubert, U. S.; Hofmeier, H. *Macromol. Rapid Commun.* **2002**, *23*, 561.
(19) Dupray, L. M.; Meyer, T. J. *Inorg. Chem.* **1996**, *35*, 6299.
(20) Kajita, T.; Leasure, R. M.; Devenney, M.; Friesen, D.; Meyer, T. J. *Inorg. Chem.* **1998**, *37*, 4782.
(21) Yoshiki, C.; Kazuki, S.; Takeo, S. *Macromolecules* **1993**, *26*, 6320.
(22) Potts, K. T.; Usifert, D. A. *Macromolecules* **1988**, *21*, 1985.
(23) Lamba, J. J. S.; Fraser, C. L. *J. Am. Chem. Soc.* **1997**, *119*, 1801.
(24) Chen, M.; Ghiggino, K. P.; Thang, S. H.; Wilson, G. J. *Angew. Chem., Int. Ed.* **2005**, *44*, 4368.
(25) Potts, K. T.; Usifer, D. A.; Guadalupe, A.; Abruna, H. D. *J. Am. Chem. Soc.* **1987**, *109*, 3961.
(26) Sprintschnik, G.; Sprintschnik, H. W.; Kirsch, P. P.; Whitten, D. G. *J. Am. Chem. Soc.* **1977**, *99*, 4947.
(27) Sullivan, B. P.; Salmon, D. J.; Meyer, T. J. *Inorg. Chem.* **1978**, *17*, 3334.
(28) Aamer, K. A.; Tew, G. N. *Macromolecules* **2007**, *40*, 2737.
(29) Johnson, R. M.; Corbin, P. S.; Ng, C.; Fraser, C. L. *Macromolecules* **2000**, *33*, 7404.
(30) Fraser, C. L.; Smith, A. P. *J. Polym. Sci., Part A: Polym. Chem.* **2000**, *38*, 4704.
(31) Wu, X.; Collins, J. E.; McAlvin, J. E.; Cutts, R. W.; Fraser, C. L. *Macromolecules* **2001**, *34*, 2812.
(32) Aamer, K. A.; Tew, G. N. *J. Polym. Sci., Part A: Polym. Chem.* **2007**, *45*, 1109.
(33) Tzanetos, N. P.; Kallitsis, J. K. *J. Polym. Sci., Part A: Polym. Chem.* **2005**, *43*, 1049.
(34) Tzanetos, N. P.; Andreopoulou, A. K.; Kallitsis, J. K. *J. Polym. Sci., Part A: Polym. Chem.* **2005**, *43*, 4838.
(35) Andreopoulou, A. K.; Kallitsis, J. K. *Eur. J. Org. Chem.* **2005**, *2005*, 4448.
(36) Chen, M.; Ghiggino, K. P.; Launikonis, A.; Mau, A. W. H.; Rizzardo, E.; Sasse, W. H. F.; Thang, S. H.; Wilson, G. J. *J. Mater. Chem.* **2003**, *13*, 2696.

10.1021/cm800911y CCC: $40.75
Published on Web 09/10/2008

the creation of coordination polymers. Terpyridine end-functionalized oligomers or well-defined polymeric chains that are afterward linked together through metal−ligand coordination bonding, forming supramolecular block copolymers, have mainly been reported by the group of Schubert.[6−8,17,18] In addition, preformed block copolymers produced by controlled polymerization techniques that are being postmodified with side tpy−Ru(II)−tpy complexes have been synthesized and extensively studied by Tew's group.[14,28,32] Initially, low metal loadings were reported, to ensure the solubility of the final hybrid material. This methodology was later extended to copolymers with higher metal loadings, using alkyl-tail-functionalized terpyridines, which further increased their solubility and self-organizational ability.[14,28] In another approach, our group reported on the synthesis of soluble homopolymers bearing side chain tpy−Ru(II)−tpy moieties. Atom transfer radical polymerization (ATRP) of a tpy-containing vinylic monomer and the subsequent complexation, using alkoxy-decorated tpy−Ru(II) monocomplexes, resulted in highly metal loaded soluble homopolymers.[33,34] All the above-mentioned approaches are mainly based on tpy ligands, and the solubility was assured either by low metal loadings[13,14] or by the use of aliphatic units either as spacers or as decorating tails.[35]

As far as the ruthenium tris(bipyridine), $[Ru^{II}(bpy)_3]^{2+}$, coordination polymeric complexes are concerned, various attempts have also been described. Polymers and copolymers with main or side chain $[Ru^{II}(bpy)_3]^{2+}$ units and their possible applications in optoelectronics have been reported.[1−3,12,17,20] Rehahn's group was the first to report on well-defined, high molecular weight, soluble coordination polymers of $[Ru^{II}(bpy)_3]^{2+}$ complexes and their UV−vis and viscosity properties.[9−11] The polymerization of $[Ru^{II}(bpy)_3]^{2+}$ complexes using reductive polymerization techniques was first described by Murray's group,[5] while copolymers where the ruthenium complexes were attached to a preformed polymeric backbone through a nucleophilic displacement were produced by the group of Meyer.[12,19,20,26] Later, Fraser's group used $[Ru^{II}(bpy)_3]^{2+}$ cores as initiators for ATRP (*divergent synthesis*) or as coupling agents of ATRP-prepared polymers (*convergent synthesis*) to produce well-defined linear and star-shaped polymers (e.g., polystyrene, poly(methyl methacrylate)),[23,29−31] a procedure also performed by Ghiggino utilizing RAFT polymerization techniques.[24,36]

However, up to now, besides the free radical polymerization (FRP)[15] and ring opening metathesis polymerization (ROMP)[16] of vinyl $[Ru^{II}(bpy)_3]^{2+}$ complexes, there have been no attempts to apply other controlled polymerization techniques, though control over molecular architecture is one of the most important scopes in this field of polymer science, since it determines to a great extent the properties of the final supramolecular material.[1−4] Especially for optoelectronic applications such as light-emitting diodes (LEDs) and photovoltaics (PVs), the charge transport and the electron donor/acceptor phase separation and interactions are the major issues determining their efficiency. Well-defined polymeric metal complexes for such applications can be prepared through controlled polymerizations of precursor polymeric chains and their complexation thereafter[6,14,16,19] or polymerization of preformed monomeric complexes.[17]

Among the different controlled polymerization techniques, the ATRP methodology[37−40] is tolerant of a number of functional groups, located on either the initiator or the vinylic monomers used, thus being a useful tool in providing homopolymers or copolymers of well-defined molecular characteristics. However, the ATRP methodology for producing homopolymers of monomeric complexes having $[Ru^{II}(bpy)_3]^{2+}$ moieties has not been presented up to now.

This work focuses on the synthesis and characterization of a vinyl-2,2′-bipyridine monomer and its resulting metal complex with Ru(II) ions and is the first report on atom transfer radical homopolymerization of such complexes using functional initiators.[33,34,41] The use of the initiators reported here will help in the further functionalization of these polymers, allowing their implementation in other reactions. As an example, the synthesized homopolymers could be introduced in polycondensation reactions or even be used in hybrid solar cells as ruthenium-containing polymeric dyes. Also FRP was applied to this new $[Ru^{II}(bpy)_3]^{2+}$ complex in combination with electron or hole transporting monomers such as oxadiazoles and carbazoles, respectively. All polymers produced were fully characterized and evaluated with respect to their structural characteristics and optical properties.

Experimental Section

Materials. Dichlorobis(2,2′-bipyridine)ruthenium(II) [*cis*-$(bpy)_2RuCl_2\cdot 2H_2O$],[26] tetrakis(triphenylphosphine)palladium $[Pd(PPh_3)_4]$,[42] 4-styrylboronic acid,[43] and 2-{4-[(4-vinylphenyl)methoxy]phenyl}-5-phenyl-1,3,4-oxadiazole[44] were produced according to the literature. 2,2′-Azobis(2-methylpropionitrile) (AIBN) was recrystallized from MeOH, diethyl ether (DEE) was distilled from Na wire, and tetrahydrofuran (THF) was distilled from Na wire in the presence of benzophenone. All other reagents and solvents were purchased by Aldrich and used as received. All reactions and polymerizations were carried out under an inert argon atmosphere.

Instrumentation. The structures of the synthesized monomers, polymers, and copolymers were clarified by high-resolution ^1H NMR and ^{13}C NMR spectroscopy with Bruker Avance DPX 400 and 100 MHz spectrometers, respectively. The samples were dissolved in deuterated chloroform ($CDCl_3$) or deuterated dimethyl sulfoxide (DMSO-d_6), using tetramethylsilane (TMS) as the internal standard.

In the case of copolymers with low metal complex content, molecular weights (M_n, M_w, PDI) were determined by gel permeation chromatography using a Polymer Laboratory chromatograph (Ultrastyragel columns with 500 and 10^4 Å pore sizes) calibrated with polystyrene standards using $CHCl_3$ (filtered through a 0.5 μm Millipore filter, analytical grade) as the eluent at a flow rate of 1 $mL\cdot min^{-1}$ at room temperature (rt) and equipped with a UV detector (254nm) along with a "Schodex RI-101" refractive index detector.

(37) Wang, J. S.; Matyjaszewski, K. *Macromolecules* **1995**, *28*, 7901.
(38) Matyjaszewski, K. *Chem.—Eur. J.* **1999**, *5*, 3095.
(39) Matyjaszewski, K.; Xia, J. *Chem. Rev.* **2001**, *101*, 2921.
(40) Kamigaito, M.; Ando, T.; Sawamoto, M. *Chem. Rev.* **2001**, *101*, 3689.
(41) Deimede, V.; Kallitsis, J. K. *Chem.—Eur. J.* **2002**, *35*, 1487.
(42) Coulson, D. R. *Inorg. Synth.* **1972**, *13*, 121.
(43) Dondoni, A.; Ghiglione, C.; Marra, A.; Scoponi, M. *J. Org. Chem.* **1998**, *63*, 9535.
(44) Tzanetos, N. P.; Kallitsis, J. K. *Chem. Mater.* **2004**, *16*, 2648.

The UV spectra were recorded on a Hitachi spectrophotometer, model U-1800. Photoluminescence spectra were obtained using a Perkin-Elmer LS45 luminescence spectrometer by excitation of the sample at the absorption maxima of the UV−vis spectra. All spectroscopic measurements were performed in quartz glass cuvettes (1 cm) at concentrations of $10^{-5}-10^{-6}$ M with respect to the repeating units. Viscosity measurements were carried out in DMF solutions with an Ostwald-type viscometer at 30 °C in a Scott Gerate AVS 310 apparatus.

Monomer Synthesis. *2-(Tributylstannyl)pyridine (**a**).* To a degassed three-necked round-bottom flask equipped with a reflux condenser, an addition funnel, and a magnetic stirrer under an argon atmosphere was added 4.25 g (2.56 mL, 26.90 mmol) of 2-bromopyridine. Through the addition funnel 50 mL of distilled DEE was added dropwise. Then the system was cooled to −80 °C followed by the dropwise addition of *n*-BuLi (1.6 M solution in *n*-hexane, 21 mL, 33.60 mmol). The reaction mixture was kept at the same low temperature for 3 h. Afterward, 9.12 mL (33.60 mmol) of tributylzinc chloride was added through the funnel, and the reaction mixture was stirred at −80 °C for another 3 h and then at rt for 12 h. Then all solvents were evaporated under vacuum, and 60 mL of distilled DEE was added. The mixture was filtered to remove any solid impurities, and the filtrate was evaporated under reduced pressure. The resulting 2-(tributylstannyl)pyridine was used in the following reaction without any further treatment. Yield: 8.41 g (85%).

*5-Bromo-2,2′-bipyridine (**b**).* To a degassed round-bottom flask equipped with a reflux condenser and a magnetic stirrer under an argon atmosphere were added 6.77 g (28.60 mmol) of 2,5-dibromopyridine and 0.66 g (0.57 mmol) of $Pd(PPh_3)_4$. The system was degassed again, and the solid from the previous reaction, 8.41 g (22.90 mmol) of 2-(tributylstannyl)pyridine, was added dissolved in 50 mL of dry xylene under an argon atmosphere. The reaction mixture was then heated at 120 °C for 14 h. After the reaction mixture was cooled to rt, 60 mL of aqueous NaOH (2 M) was added. The mixture was extracted with toluene and dried over $MgSO_4$. The solvent was evaporated under vacuum, and the crude solid product was purified via column chromatography (silica gel, 230−400 mesh, ASTM) using *n*-hexane/ethyl acetate (5:1) as the eluent. The desired product was obtained as a white crystalline powder which was dried at 45 °C under vacuum. Yield: 3.51 g (65%). ^{1}H NMR ($CDCl_3$): 7.33 (ddd, 1H), 7.82 (td, 1H), 7.94 (dd, 1H), 8.32 (d, 1H), 8.37 (d, 1H) 8.67 (dt, 1H), 8.72 (d, 1H) ppm. ^{13}C NMR ($CDCl_3$): 120.92, 121.09, 122.29, 123.96, 136.97, 139.45, 149.21, 150.15, 154.58, 155.13 ppm.

*5-(*p*-Vinylphenyl)-2,2′-bipyridine (**c**).* To a degassed three-necked round-bottom flask equipped with a reflux condenser, an addition funnel, and a magnetic stirrer under an argon atmosphere were added 0.80 g (3.40 mmol) of 5-bromo-2,2′-bipyridine, 0.75 g (5.10 mmol) of 4-styrylboronic acid, and 0.15 g (0.13 mmol) of $Pd(PPh_3)_4$. The system was degassed again, and 70 mL of distilled THF and 6.37 mL of K_2CO_3 (2 M) degassed aqueous solution were added. The reaction mixture was refluxed for 48 h. After being cooled to rt, the mixture was extracted using toluene and dried over $MgSO_4$. The solvent was removed under vacuum, the resulting yellow solid was stirred for 2 h in *n*-hexane and filtered to remove any impurities, and the filtrate was evaporated. A white powder was obtained after the residue was dried under reduced pressure at 30 °C for 24 h. Yield: 0.75 g (85%). Purity by ^{1}H NMR: 90%. The product was further purified via column chromatography (silica gel, 230−400 mesh, ASTM) using dichloromethane, which elutes the impurities, and then dichloromethane/MeOH (20:1), which elutes the desired clean product. The yield by chromatography was 85%, and the purity of the product was estimated as 100% by ^{1}H NMR spectroscopy. ^{1}H NMR ($CDCl_3$): 5.32 (d, 1H), 5.83 (d, 1H), 6.78 (q, 1H), 7.33 (ddd, 1H), 7.53 (d, 2H), 7.63 (d, 2H), 7.84 (td, 1H), 8.03 (dd, 1H), 8.45 (q, 2H), 8.71 (d, 1H) 8.93 (d, 1H) ppm.

Scheme 1. Synthetic Route toward [5-(*p*-Vinylphenyl)-2,2′-bipyridine]bis(2,2′-bipyridine)ruthenium(II), $[Ru(vbpy)(bpy)_2](PF_6)_2$ (d)

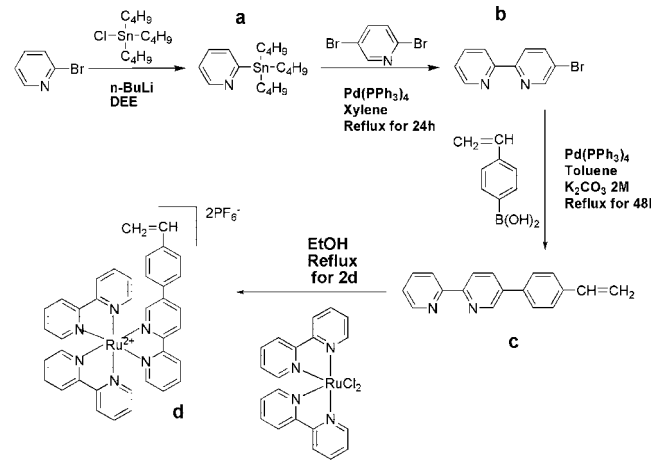

*[5-(*p*-Vinylphenyl)-2,2′-bipyridine]bis(2,2′-bipyridine)ruthenium(II), $[Ru^{II}(vbpy)(bpy)_2](PF_6)_2$ (**d**).* To a degassed round-bottom flask equipped with a reflux condenser and a magnetic stirrer under an argon atmosphere were added 0.12 g (0.47 mmol) of **c**, 0.16 g (0.31 mmol) of $[cis\text{-}(bpy)_2RuCl_2\cdot 2H_2O]$,[26] and 30 mL of absolute EtOH. The reaction mixture was degassed once again and refluxed for 72 h. The resulting red-colored mixture was cooled to rt, and the solvent was evaporated under reduced pressure, affording an orange powder. Afterward 40 mL of deionized water was added, and the mixture was stirred for 0.5 h, followed by filtration to remove solid impurities. To the filtrate was added 20 mL of an aqueous solution of NH_4PF_6, which caused the formation of orange crystals to precipitate spontaneously. The crystals formed were filtered and washed with deionized water to remove the excess NH_4PF_6 and consecutively with DEE. Drying under vacuum at 45 °C for 24 h afforded the final product. Yield: 0.270 g (87%). ^{1}H NMR (DMSO-d_6): 5.33 (d, 1H), 5.94 (d, 1H), 6.75 (q, 1H), 7.46 (d, 2H), 7.51−7.58 (m, 7H), 7.71−7.78 (m, 4H), 7.86 (d, 1H), 7.91 (d, 1H), 8.14−8.23 (m, 5H), 8.51 (dt, 1H), 8.79−.92 (m, 6H) ppm. ^{13}C NMR (DMSO-d_6): 116.57, 124.92, 124.97, 125.05, 125.14, 127.53, 127.61, 128.27, 128.32, 128.46, 134.03, 135.82, 136.12, 138.43, 138.76, 138.88, 148.39, 151.70, 152.16, 152.30, 155.71, 156.82, 156.91, 157.02, 157.12, 157.21 ppm.

Polymerizations. *Atom Transfer Radical Polymerization using Functional Initiators.* A round-bottom flask equipped with a rubber septum, a magnetic stirrer, and a gas inlet/outlet was flamed under vacuum. Initiator 5-[[4-(bromomethyl)benzyl]oxy]benzene-1,3-dioic acid (**Ia**),[33,41] 5.72 mg (0.02 mmol), or the distyrylanthrcene derivative **II**,[34] 11.94 mg (0.02 mmol) (shown in Schemes 2 and 3), was added to the flask which contained CuBr, 5.75 mg (0.04 mmol), and 8.4 μL (0.04 mmol) of *N*,*N*,*N*′,*N*″,*N*″-pentamethyldiethylenetriamine (PMDETA). The system was degassed three times and flushed with argon. The solvent dimethyl formamide (DMF) and 385 mg (0.4 mmol) of monomer **d** were added to the flask, and the mixture was immediately degassed and flushed with argon three times. The reaction mixture was then immersed in an oil bath and heated at 110 °C for 24 h. After the reaction mixture was cooled to room temperature, 2 mL of DMF was added to dissolve the polymer. The suspension was filtered from silica gel to remove most of the catalyst. The resulting polymer was precipitated as a dark-orange crystalline-like powder in 20-fold excess by volume of methanol. Filtration and excessive washing

Scheme 2. Atom Transfer Radical Polymerization of Monomer d and Its Kinetic Study (I/M versus Time)

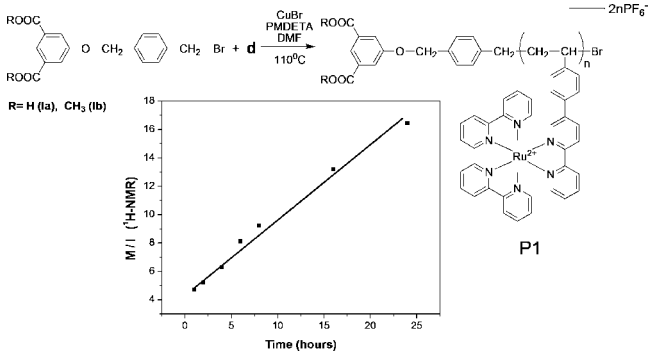

Table 1. Characterization of Polymers P1 and P2

polymer	feed ratio, initiator/ monomer	no. of monomers attached	M_n estimation by ^{1}H NMR	η_{red}[a] at $C = 0.5$ mg/mL
P1a	1/05	7	~7100	
P1b	1/10	9	~9000	
P1c	1/10	10	~10000	
P1d	1/10	13	~12900	41.77
P1e	1/15	16	~16300	
P2a	1/06			11.19
P2b	1/10			21.92
P2c	1/20			51.80

[a] In DMF at 30 °C.

with MeOH and DEE removed any remaining impurities. The final polymeric material was dried under vacuum at 45 °C overnight. The results for the different prepared polymers are summarized in Table 1. ^{1}H NMR (DMSO-d_6) for polymers **P1**: 3.90 (s), 4.55(s), 5.30 (s), 7.55 (br), 7.74 (br), 7.95 (br), 8.17 (br), 8.81 (br) ppm. ^{1}H NMR (DMSO-d_6) for polymers **P2**: 6.87 (br), 7.54 (br), 7.74 (br), 7.95 (br), 8.17 (br), 8.81 (br) ppm.

Free Radical Polymerization: General Procedure. To a degassed round-bottom flask equipped with a magnetic stirrer and a gas inlet/outlet were added the desired amounts of monomer **d** and of oxadiazole monomer (2-{4-[(4-vinylphenyl)methoxy]phenyl}-5-phenyl-1,3,4-oxadiazole, OXD) or carbazole monomer (9-vinylcarbazole, CARB), along with the respective amounts of AIBN. Then 3 mL of DMF was added, and the system was flushed with argon and immersed into an oil bath at 110 °C for 4 days. Then the reaction mixture was allowed to cool at room temperature and was precipitated in 20-fold excess by volume of the solvent required in each case.

For copolymers **P3**, the synthesis of **P3iv** (feed ratio 15/85 OXD/monomer **d**) is presented as an example: A 16 mg (0.042 mmol) portion of the OXD monomer and 240 mg (0.250 mmol) of monomer **d** were added to the flask along with 1.23 mg (0.003 mmol) of AIBN and 3 mL of DMF. The reaction mixture was immersed into an oil bath at 110 °C for 4 days and then precipitated in 60 mL of methanol. Depending on the molar ratio of the copolymers, they were precipitated in methanol or methanol/ethyl acetate or methanol/water mixtures as the percentage of the oxadiazole unit increased, respectively. After filtration the polymers were further washed with methanol and ethyl acetate, to remove any excess of monomers, and consecutively with DEE and dried under vacuum at 45 °C overnight. The copolymers obtained were further purified by reprecipitation from $CHCl_3$ or acetonitrile in DEE. The results are summarized in Table 2. ^{1}H NMR (DMSO-d_6) for copolymers **P3**: 1.5−2.4 (br, 3H of **d** plus 3H of OXD), 4.9 (br, 2H of OXD), 6.2−8.3 (br, 20H of **d** plus 13H of OXD), 8.4−8.9 (br, 7H of **d**) ppm.

Table 2. Molecular Characteristics of Copolymers P3

copolymer, OXD/Ru	composition, ^{1}H NMR	M_n[a]	M_w[a]	PDI[a]
P3i, 95/5	96/04	3100	6900	2.20
P3ii, 90/10	94/06	4100	5100	1.25
P3iii, 85/15	86/14	2700	3200	1.20
P3iv, 75/25	80/20			
P3v, 50/50	60/40			
P3vi, 15/85	22/78			
P3vii, 10/90	13/87			

[a] M_n, M_w, and PDI (M_w/M_n) from GPC measurements using $CHCl_3$ as the eluent and polystyrene standards.

Table 3. Molecular Characteristics of Copolymers P4

copolymer, CARB/Ru	composition,^{1}H NMR	M_n[a]	M_w[a]	PDI[a]
P4i, 95/5	90/10	17400	22300	1.30
P4ii, 85/15	73/27	14500	19300	1.35
P4iii, 75/25	67/33	29100	47600	1.65
P4iv, 50/50	54/46			
P4v, 25/75	33/67			
P4vi, 15/85	23/77			
P4vii, 10/90	14/86			

[a] M_n, M_w, and PDI (M_w/M_n) from GPC measurements using $CHCl_3$ as the eluent and polystyrene standards.

For the **P4** copolymers an example for the synthesis of **P4iv** (for a feed ratio of 50/50 CARB/monomer **d**) is presented: A 29 mg (0.015 mmol) portion of the CARB monomer and 144 mg (0.015 mmol) of monomer **d** were added to the flask along with 1.23 mg (0.003 mmol) of AIBN. The system was degassed and flushed with argon again. Then 3 mL of DMF was added, and the reaction mixture was immersed in an oil bath at 110 °C for 4 days. The copolymers were obtained by precipitation in 20-fold excess by volume of methanol and were further purified by reprecipitation from $CHCl_3$ or acetonitrile in DEE. The results are summarized in Table 3. ^{1}H NMR (DMSO-d_6) for copolymers **P4**: 1.5−2.4 (br, 3H of **d** plus 3H of CARB), 5.7−8.3 (br, 20H of **d** plus 13H of CARB), 8.6−8.9 (br, 7H of **d**) ppm.

Results and Discussion

The synthesis of the vinylic ruthenium complex **d** (Scheme 1) was based on the novel vinylphenyl-2,2′-bipyridine monomer **c**, produced from the brominated bipyridine derivative **b**.[45−54] The synthesis of monobromobipyridine derivatives in the past, was mainly based on bromination under harsh reaction conditions,[47] resulting in low yields. Recently the use of stannyl reagents has provided another way to produce these derivatives in better yields and under milder conditions.[45] In this work, for producing derivative **b**, we employed a procedure slightly modified with respect to the use of (trimethylstannyl)pyridine,[45] by utilizing 2-(tributylstannyl)pyridine (**a**) under the same mild condi-

(45) Schwab, P. F. H.; Fleischer, F.; Michl, J. *J. Org. Chem.* **2002**, *67*, 443.
(46) Smith, A. P.; Corbin, P. S.; Fraser, C. L. *Tetrahedron Lett.* **2000**, *41*, 2787.
(47) Romero, F. M.; Ziessel, R. *Tetrahedron Lett.* **1995**, *36*, 6471.
(48) Zoltewicz, J. A.; Cruskie, M. P., Jr *Tetrahedron* **1995**, *51*, 11393.
(49) El-ghayoury, A.; Ziessel, R. *J. Org. Chem.* **2000**, *65*, 7757.
(50) Malm, J.; Bjoerk, P.; Gronowitz, S.; Hörnfeldt, A. B. *Tetrahedron Lett.* **1992**, *33*, 2199.
(51) Peters, D.; Hörnfeldt, A. B.; Gronowitz, S. *J. Heterocycl. Chem.* **1990**, *27*, 2165.
(52) Miyaura, N.; Suginome, H.; Suzuki, A. *Tetrahedron* **1983**, *39*, 3271.
(53) Miyaura, N.; Ishiyama, T.; Ishikawa, M.; Suzuki, A. *Tetrahedron Lett.* **1986**, *27*, 6369.
(54) Savage, S. A.; Smith, A. P.; Fraser, C. L. *J. Org. Chem.* **1998**, *63*, 10048.

Scheme 3. Molecular Representation of Polymers P1 and P2[a]

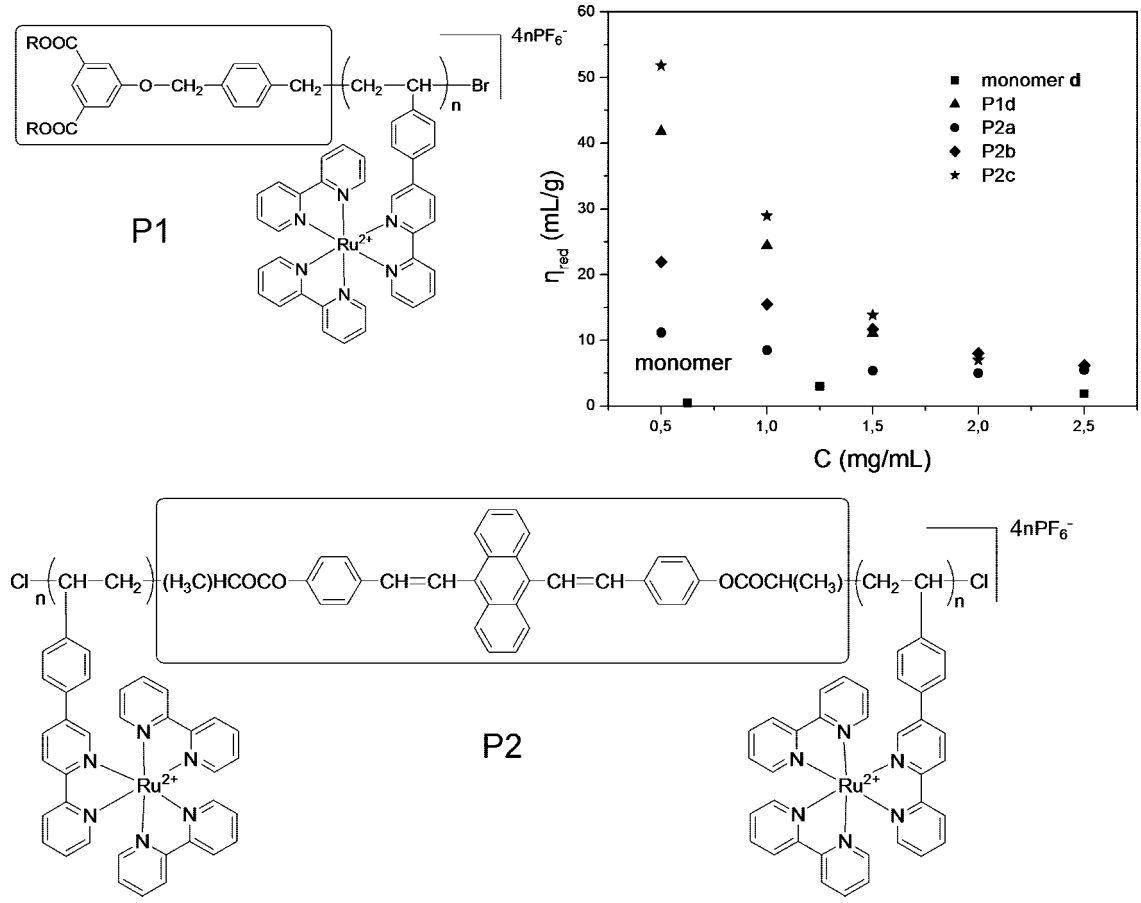

[a] The frames show the initiators used. Inset: viscosity measurements for **P1d** (▲), **P2a** (●), **P2b** (◆), **P2c** (★), and monomer **d** (■) in DMF at 30 °C.

tions. Taking advantage of the Stille coupling reaction[45,48,53] between compound **a** and 2,5-dibromopyridine, combined with the different reactivities between the bromine atoms, we obtained higher yields for the desired monobromobipyridine **b**. As a consequence, the vinylbipyridine monomer **c** was produced via a Suzuki coupling reaction[45,52,53] between compound **b** and 4-styrylboronic acid.[43] Finally the vinyl complex monomer **d** was produced after a complexation reaction of compound **c** with dichlorobis(2,2′-bipyridine)ruthenium(II),[26] followed by counterion exchange from a saturated aqueous solution of NH_4PF_6. Clarification of its chemical structure was performed by ^1H and ^{13}C NMR spectroscopy (Figure 1; see also the Experimental Section).

Homopolymers of monomer **d** were synthesized via ATRP using functional or chromophoric initiators (**Ia**, dicarboxylic acid, and **Ib**, dicarboxylic acid methyl ester,[33,41] or the distyrylanthracene **II** derivative,[34] respectively, Schemes 2 and 3). On the other hand, free radical copolymerization of monomer **d** with oxadiazole or carbazole monomers resulted in electron/hole transporting polymeric architectures (Figures 3 and 4).

In particular, using different initiators (monofunctional **Ia** and **Ib** and bifunctional **II**) and the $[Ru(vbpy)(bpy)_2](PF_6)_2$ unit (**d**), we performed controlled ATR polymerizations that produced well-defined, easily soluble homopolymeric (**P1**) and polymeric triblock (**P2**) complexes. Monomer **d** and the synthesized polymers were characterized via ^1H NMR,

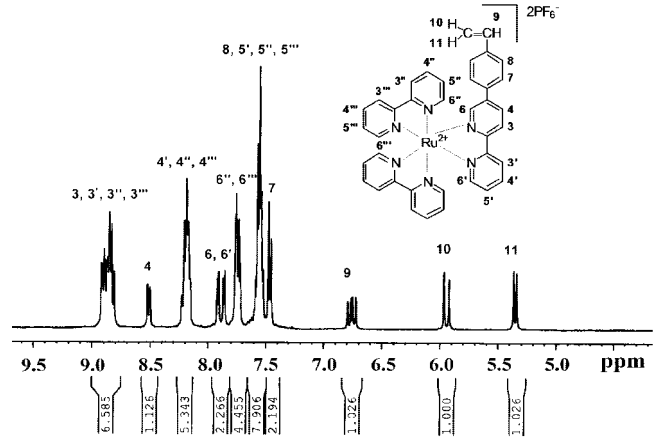

Figure 1. ^1H NMR spectra of monomer **d** in DMSO-d_6.

UV−vis, and photoluminescence (PL) spectroscopy. These polymeric complexes exhibit excellent solubility properties in polar nonprotic solvents, such as acetone, CH_3CN, DMF, and DMSO. The functional initiators of **P1** homopolymers, having dicarboxylic acid methyl ester or dicarboxylic acid functionalities, allow the design and synthesis of more complex architectures (e.g., comb- or starlike structures) since they can be utilized in subsequent reactions such as polycondensations or they can even be directly applied in hybrid solar cells. Additionally all copolymers produced by the FRP

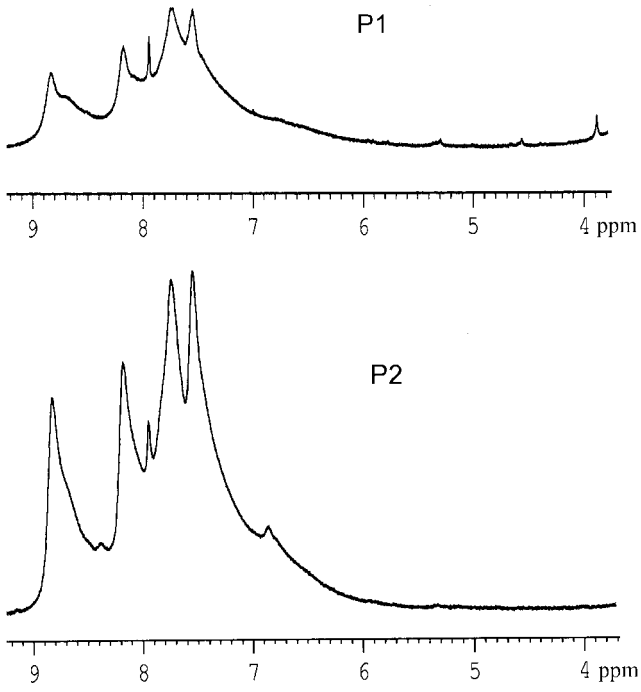

Figure 2. ^{1}H NMR spectrum of polymers **P1** and **P2** in DMSO-d_6.

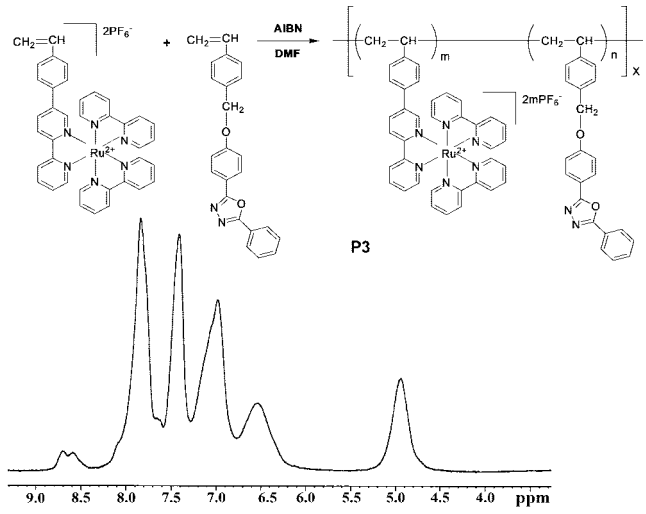

Figure 3. Synthesis of copolymers **P3** and ^{1}H NMR spectrum of **P3iv** in DMSO-d_6.

technique exhibit the same solubility properties and were similarly characterized.

On the basis of the ^{1}H NMR spectra of polymers **P1** and **P2**, shown in Figure 2, the successful ATR polymerization is proved, since the olefins' peaks at 5.33, 5.94, and 6.75 ppm of the bpy monomer are not present. The case of thermal polymerization is also excluded, since the protons of the initiators are evident. Thus, in the case of **P1**, as shown in Figure 2, the peaks at 3.90, 4.55, and 5.30 ppm attributed to the methyl and methylene protons of the initiator **Ia** can be used to calculate the polymers' M_n. The results of these calculations are presented in Table 1, showing the close agreement between the feed ratio of initiator to monomer and the calculated M_n. This is another piece of evidence of a successful ATR polymerization and not just a conventional radical or thermal polymerization. Moreover, to prove the

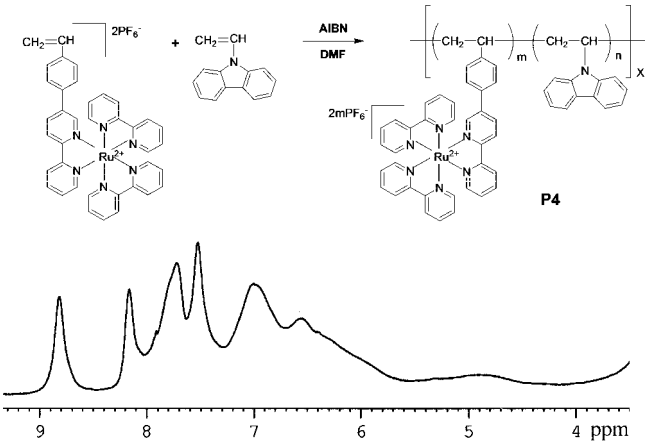

Figure 4. Synthesis of copolymers **P4** and ^{1}H NMR spectrum of **P4ii** in DMSO-d_6.

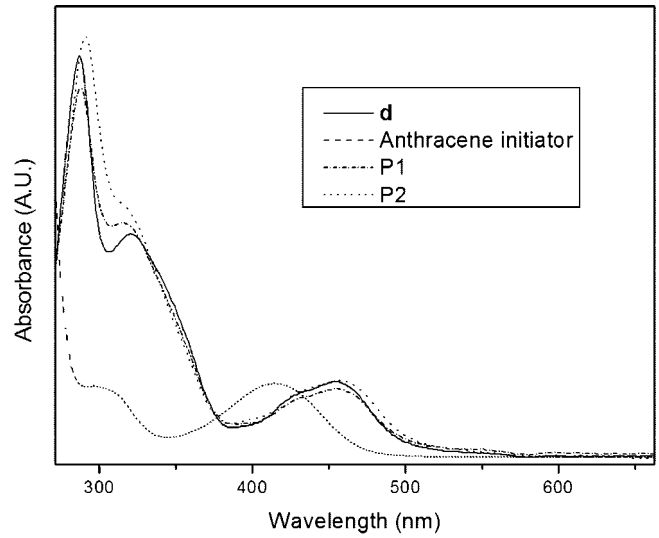

Figure 5. UV−vis absorption spectra of monomer **d**, polymers **P1** and **P2**, and the anthracene initiator **II** used in **P2** in DMF.

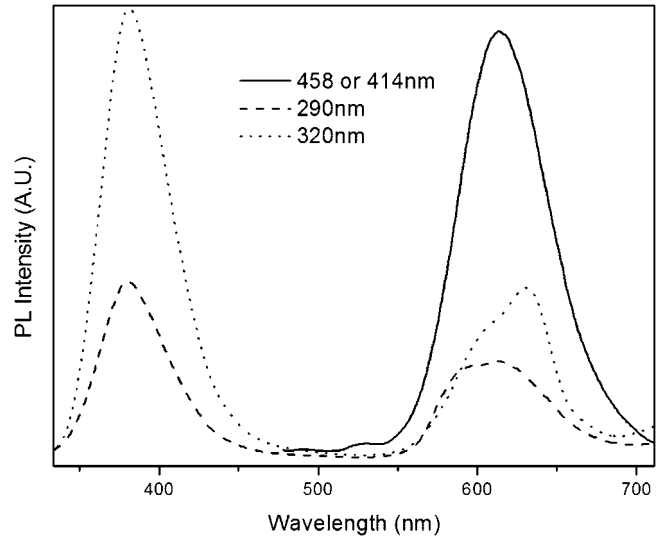

Figure 6. PL spectra of polymer **P2** after excitation at λ = 290, 320, and 458 nm in DMF.

controlled character of these polymerizations, we performed kinetic studies that were carried out analogously to the general polymerization procedure. We selected the monomer

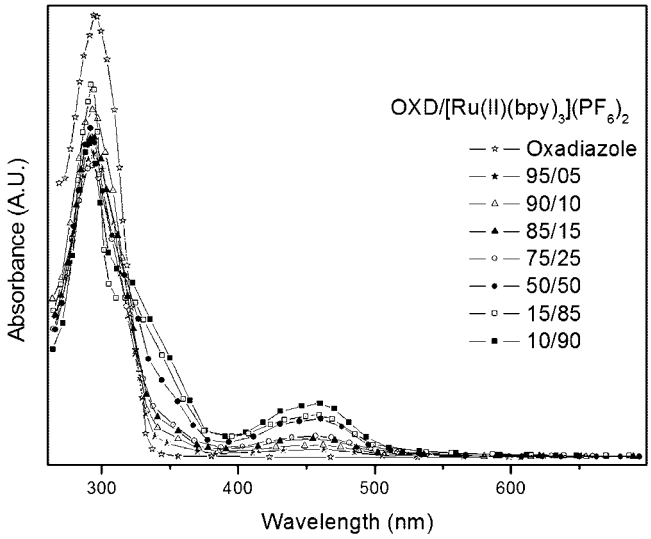

Figure 7. UV−vis absorption spectra of copolymers **P3** and of the oxadiazole monomer in DMF.

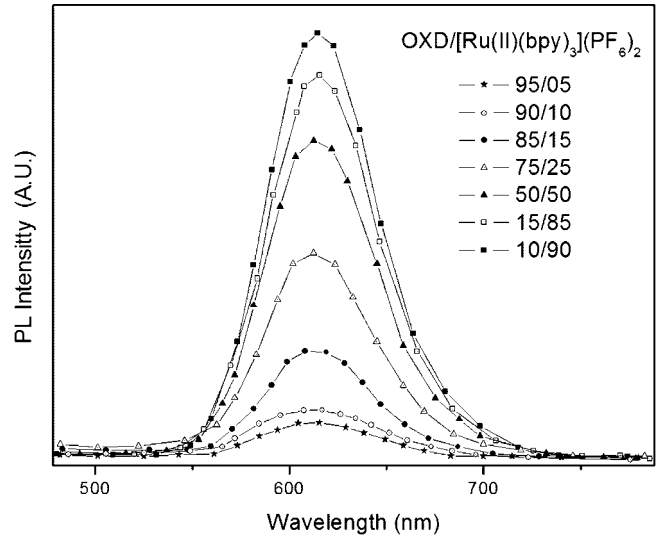

Figure 9. PL spectra of copolymers **P3** after excitation at $\lambda = 458$ nm in DMF.

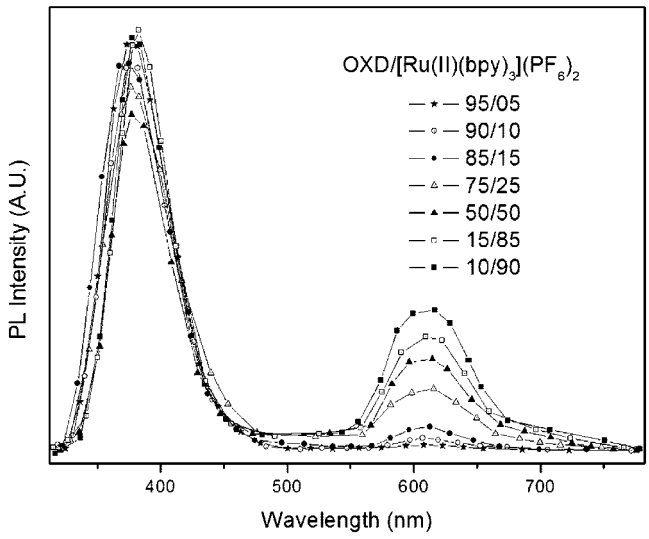

Figure 8. PL spectra of copolymers **P3** after excitation at $\lambda = 290$ nm in DMF.

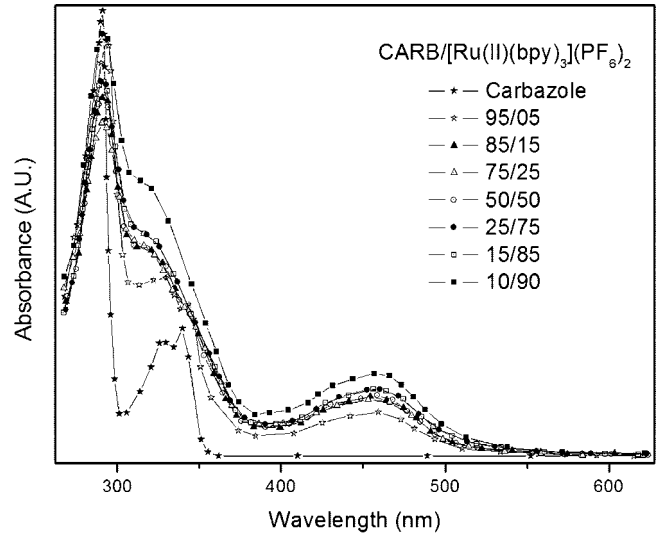

Figure 10. UV−vis absorption spectra of copolymers **P4** and of the carbazole monomer in DMF.

d/initiator **Ia**/CuBr/PMDETA (15/1/2/2) system for a kinetic study. During the reaction time, seven samples of 0.30 mL were withdrawn, and each one was precipitated in 20 mL of deionized water. This way, the catalytic complex of copper/PMDETA was diluted; the samples were centrifuged and washed again with water three times. Finally the same procedure was repeated three times with diethyl ether to remove any trace of unreacted initiator. Thus, the ^{1}H NMR end group analysis technique was used to estimate the true M_n values of our polymers during the polymerization. The M_n values were determined by ^{1}H NMR spectroscopy from the signal at $\delta = 3.9$ ppm corresponding to the methyl protons of the **Ia** initiator used (6 protons) and the whole region from 7.3 to 8.9 ppm corresponding to the aromatic protons of both the monomer (27 protons) and the polymer (27 protons). A representative ^{1}H NMR spectrum of the α-dicarboxylic acid methyl ester **Ib** initiated polymer **P1** for the kinetic study, with the assignment of all peaks, is depicted in the Supporting Information (Figure S1). The plot of initiator monomer (M)/(I) versus time is linear, indicating that the number of growing radicals remained constant throughout the polymerization (Scheme 2). Concerning polymer **P2**, there are no selective peaks for both the initiator **II** and the polymer to obtain the M_n value through the ^{1}H NMR technique in this case.

For the copolymers of the ruthenium complex with oxadiazole units (**P3**), the composition ratio could be calculated from the ^{1}H NMR spectra, since selective peaks can be observed. Composition calculations were based on the ^{1}H NMR peak at 8.4−8.9 ppm, attributed to six of the bpy aromatic protons of the $[Ru(vbpy)(bpy)_2]^{2+}$ unit, and the peak at 5.0 ppm, attributed to the methylene protons in the α-position to the oxygen atom of the side oxadiazole unit (Figure 3).

In the case of copolymers of the ruthenium complex with carbazole units (**P4**), the composition ratio could once again be estimated by the ^{1}H NMR spectra, though roughly, due to the low discrimination of the respective monomers and

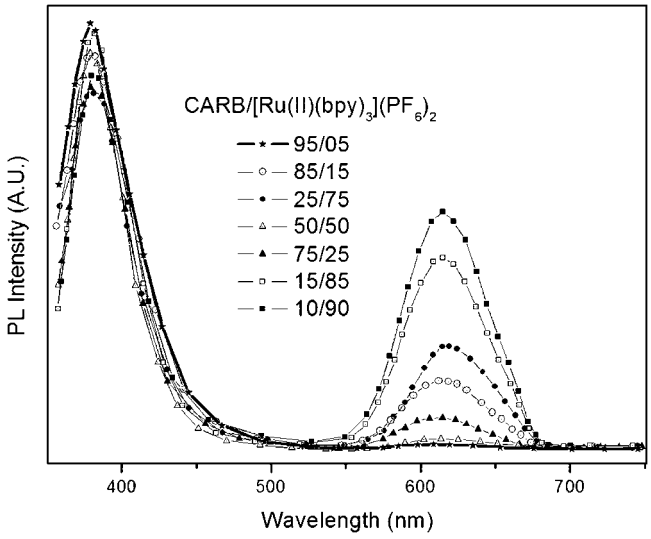

Figure 11. CARB/[Ru(II)(bpy)$_3$](PF$_6$)$_2$: 95/05 = ★, 85/15 = △, 75/25 = ▲, 50/50 = ○, 25/75 = ●, 15/85 = □, 10/90 = ■.

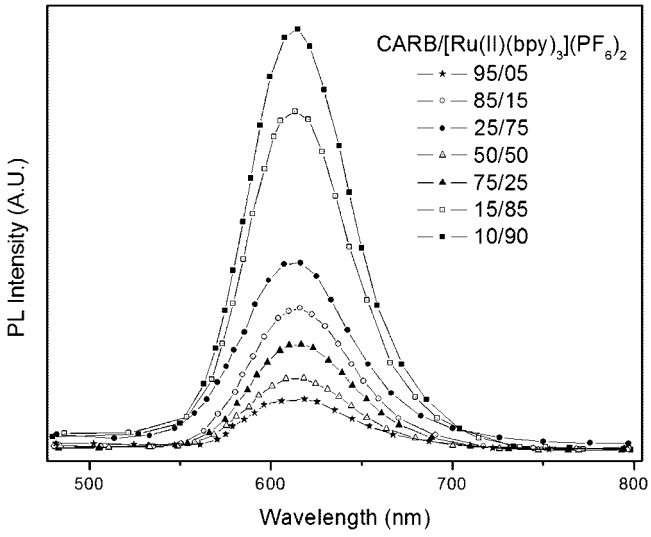

Figure 12. CARB/[Ru(II)(bpy)$_3$](PF$_6$)$_2$: 95/05 = ★, 85/15 = △, 75/25 = ▲, 50/50 = ○, 25/75 = ●, 15/85 = □, 10/90 = ■.

the broadness of the spectrum peaks. The ^{1}H NMR peak at 8.4−8.9 ppm, attributed to six of the bpy aromatic protons of the [Ru(vbpy)(bpy)$_2$]$^{2+}$ unit, and the broad peak from 5.6−7.3 ppm, attributed to six aromatic protons of the carbazole unit, were used for this estimation (Figure 4).

In an attempt to calculate the homopolymers' **P1** and **P2** molecular characteristics (M_n, M_w, PDI), we tried to perform GPC measurements with UV detection at 254 nm. This was unsuccessful, which is justified according to the literature,[15,16,28] since there are strong interactions of the ruthenium complexes with the polystyrene stationary phase of GPC columns. However, there are examples of successful GPC characterization of metal-containing polymers with comparatively low metal loading.[6,21,24,36] In our case, the high metal complex loadings of most of our polymers did not allow their characterization using GPC. Despite that, to prove once again the polymeric nature of these complexes, viscometric characterization was applied.[10,11,35] These measurements were performed for **P1**, **P2**, and **d** in DMF at 30 °C, and the results are summarized in Table 1. In addition, the inset in Scheme 3 shows the viscosity values obtained for polymers **P1d**, **P2a**−**c**, and monomer **d** for different concentrations; an increase in the reduced viscosity values is evident as the solution concentration decreases. Such a behavior can be explained in terms of the polyelectrolyte nature of the polymers due to the presence of Ru(II) and the PF_6^- counterions. Comparison of the viscosity values with those of the vinylic monomer **d**, as well as the relation of the viscosity value of polymer **P1d** with the M_n value obtained by ^{1}H NMR, fully supports the formation of polymeric hybrid materials in both the cases of **P1** and **P2**.

On the other hand, the copolymers of ruthenium complexes with oxadiazole units (**P3**) could be successfully characterized with GPC, but only for those having low metal loadings (less interaction with the polystyrene columns used). It was observed that in the cases of higher oxadiazole loadings (feed composition ratios of 95/05, 90/10, and 85/15) the copolymers were soluble in $CHCl_3$ and their GPC characterization was possible, as shown in Table 2. A representative GPC trace of **P3iii** copolymer is provided in the Supporting Information (Figure S2). Similarly, for the **P4** copolymers, GPC characterization was successful for high carbazole loadings (feed composition ratios of 95/05, 85/15, and 75/25), as shown in Table 3. A representative GPC trace of **P4iii** copolymer is provided in the Supporting Information (Figure S3) as well.

Optical Characterization. The [Ru(vbpy)(bpy)$_2$](PF$_6$)$_2$ unit (**d**), homopolymers **P1** and **P2**, and copolymers **P3** and **P4** were thoroughly characterized with respect to their optical properties in dilute DMF solutions (10^{-5}−10^{-6} M), via UV−vis and PL spectroscopies. In all cases the characteristic absorption and emission bands of the [Ru^{II}(bpy)$_3$]$^{2+}$ complexes were observed. On the other hand, for copolymers **P3** and **P4**, bands due to the synergistic effect of both the monomer **d** and OXD or CARB coexisting moieties could be detected, with varying intensities depending on the ratios of the comonomers. All homopolymers and copolymers present intense red light emissions.

Concerning the monomer **d** and the polymers **P1** and **P2**, UV−vis spectroscopy revealed identical spectra, exhibiting an absorption peak at around λ = 292 nm and a "shoulder" at λ = 320 nm, attributed to $\pi-\pi^*$ LC (ligand-centered) transitions of 2,2′-bipyridine, and an absorption maximum at λ = 458 nm, which is characteristic of the d−π^* MLCT (metal to ligand charge transfer) of the [Ru(vbpy)(bpy)$_2$](PF$_6$)$_2$ complexes (Figure 5). In the case of **P2**, where the anthracene unit is used as the initiator, one should expect an additional absorption peak at λ = 414 nm attributed to the anthracene unit, as shown in Figure 5, but particularly this peak is overlapped by the ruthenium complex absorption at 458 nm, since the concentration of the anthracene initiator in **P2** is very low.

Photoluminescence investigation of monomer **d** and polymers **P1** and **P2** after excitation at λ = 290 nm and λ = 320 nm revealed identical emission peaks located at around λ = 380 nm and λ = 615 nm attributed to the [Ru(vbpy)(bpy)$_2$](PF$_6$)$_2$ complex. Depending on the excitation wavelength, varying emission intensities were observed as

shown in Figure 6. Additionally, in the case of **P2**, due to the overlapping of the absorption band of monomer **d** and the anthracene moiety, after being excited either at $\lambda = 414$ nm (where the absorption maxima of the anthracene initiator is located) or at $\lambda = 458$ nm (attributed to monomer **d**), emissions at $\lambda = 520$ nm and $\lambda = 615$ nm were observed, proving the incorporation of the anthracene group along the polymeric backbone (Figure 6).

The UV−vis optical characterization of copolymers **P3** revealed similarities with those of polymers **P1** and **P2**. As shown in Figure 7, the d−π* MLCT absorption band of the $[Ru(vbpy)(bpy)_2](PF_6)_2$ unit is evident at $\lambda = 458$ nm. Moreover, **P3** copolymers exhibit a peak of higher intensity, with maxima either at $\lambda = 296$ nm (absorption maxima of the oxadiazole unit) or at $\lambda = 292$ nm (absorption of bpy ligands), plus a shoulder at around $\lambda = 320$ nm attributed to the $\pi-\pi$* LC transition of 2,2′-bipyridines, depending on the molar ratio of the copolymer. In that order, the absorption maxima observed for **P3i**−**vii** vary from 296 to 292 nm, whereas the shoulder at $\lambda = 320$ nm is observed only in cases of high metal loadings. Furthermore, it should be outlined that the intensity of the MLCT absorption band at 458 nm increases by increasing the ratio of the metal complex to the copolymer, whereas the absorption band at ∼294 nm remains relatively constant.

Photoluminescence spectra of copolymers **P3** were obtained after excitation at $\lambda = 290$ nm and $\lambda = 458$ nm with emission maxima at $\lambda = 382$ nm and $\lambda = 615$ nm (Figures 8 and 9). The first peak is attributed to the $\pi-\pi$* LC absorption band of both 2,2′-bipyridine and the oxadiazole unit, while the latter is characteristic only of the d−π* MLCT absorption band of the $[Ru(vbpy)(bpy)_2](PF_6)_2$ unit.

Concerning copolymers **P4**, their optical properties resemble those of **P3**. In the UV−vis spectra of copolymers **P4i**−**vii**, one can observe absorption peaks at $\lambda = 458$ nm characteristic of the d−π* MLCT absorption band of the $[Ru(vbpy)(bpy)_2](PF_6)_2$ unit as shown in Figure 10. Moreover, **P4** copolymers exhibit a peak of higher intensity, with a maximum located at $\lambda = 292$ nm and a shoulder at around $\lambda = 320$ nm, originating from the $\pi-\pi$* LC transition of 2,2′-bipyridine, as well as the carbazole units. Furthermore, it should be pointed out that the absorption intensity of the MLCT band increases compared to that at ∼292 nm, similarly to that of **P3**, by increasing the ratio of the metal complex to the copolymer.

Photoluminescence spectra of **P4** were obtained after excitation at $\lambda = 290$ nm (Figure S4, Supporting Information), $\lambda = 340$ nm (Figure 11), and $\lambda = 458$ nm (Figure 12). Emission peaks were observed at $\lambda = 382$ nm and $\lambda = 615$ nm. The first peak is attributed to the $\pi-\pi$* LC absorption band of 2,2′-bipyridine and to the carbazole unit, while the latter is characteristic of the d−π* MLCT absorption band of the $[Ru(vbpy)(bpy)_2](PF_6)_2$ unit. All copolymers **P4i**−**vii** exhibit similar spectral characteristics after excitation at the absorption maxima of the carbazole and the bipyridine unit at ∼290 nm. The emission wavelength range consists of bands at $\lambda = 380$ nm and $\lambda = 615$ nm. If excitation takes place at $\lambda = 340$ nm, where the carbazole moiety absorbs, the same emission bands appear (Figure 11). When the excitation wavelength is 458 nm, only emission peaks at $\lambda = 615$ nm are observed (Figure 12). All of the above optical data ensure the incorporation of the $[Ru(vbpy)(bpy)_2](PF_6)_2$ unit into the polymeric chains and the ability of these types of polymers and copolymers to incorporate the optical properties of the metallic complex.

Conclusions

The newly developed vinylbipyridine monomer **c** used in this work was synthesized from bromopyridine derivatives, taking advantage of the combination of Stille and Suzuki palladium-catalyzed coupling reactions. Complexation of this monomer with ruthenium ions resulted in the high-yield preparation of the $[Ru(vbpy)(bpy)_2](PF_6)_2$ complex (**d**). This vinylic complex was successfully employed in atom transfer radical polymerization, demonstrating for the first time the ability of such complexes to be polymerized via ATRP. Moreover, it was copolymerized via FRP with oxadiazole and carbazole monomers, producing copolymers with electron/hole transporting architectures, respectively. All polymers and copolymers were soluble in common organic solvents, despite their high metal loadings. A complete characterization via ^{1}H NMR, GPC, and viscosity measurements was performed. On the basis of the "architecture" of these polymers and copolymers, and their optical characteristics (UV−vis and PL), applications in optoelectronic devices seem quite feasible. The key advantage of this work, besides the high-yield synthesis of the new vinyl monomer **d**, is its direct ATR homopolymerization, using various functional initiators. These homopolymers bearing $[Ru^{II}(bpy)_3]^{2+}$ complexes on every single repeating unit were easily soluble in common organic solvents, allowing their thorough characterization with respect to their structural and optical characteristics. Moreover, the combination of the optical characteristics of the metal complex with the polymers' properties and more importantly with the electron or hole transporting characteristics of the comonomers employed is expected to further contribute to the balanced charge mobility of these materials.

Acknowledgment. Financial support for this project from the Greek Ministry of Development under Research Grant PENED 03ED118 "Organic Solar Cells" is gratefully acknowledged. This research project (PENED) is cofinanced by the EU European Social Fund (75%) and the Greek Ministry of Development, GSRT (25%).

Supporting Information Available: A representative ^{1}H NMR spectrum of the ATRP kinetic study of **P1e** along with GPC traces of **P3iii** and **P4iii** copolymers and the PL spectrum of copolymers **P4** after excitation at 290 nm. This material is available free of charge via the Internet at http://pubs.acs.org.

CM800911Y

Carbon Nanotubes Decorated with Terpyridine-Ruthenium Complexes

ANDREAS A. STEFOPOULOS,[1,2] ELEFTHERIOS K. PEFKIANAKIS,[1] KONSTANTINOS PAPAGELIS,[3] AIKATERINI K. ANDREOPOULOU,[1] JOANNIS K. KALLITSIS[1,2]

[1]Department of Chemistry, University of Patras, GR-26500 Rio-Patras, Greece

[2]Foundation of Research and Technology Hellas, Institute of Chemical Engineering and High Temperature Processes, GR-26500 Rio-Patras, Greece

[3]Department of Materials Science, University of Patras, 26504 Rio-Patras, Greece

Received 13 January 2009; accepted 5 February 2009
DOI: 10.1002/pola.23339
Published online in Wiley InterScience (www.interscience.wiley.com).

ABSTRACT: Surface functionalization of CNTs (SWCNTs or MWCNTs) with dendronized alkoxy terpyridine-Ru(II)-terpyridine complexes has been accomplished using either the "grafting to" or the "grafting from" approaches. Different sets of easily processable hybrid metallo-CNTs composites have been efficiently synthesized bearing either monomeric or polymeric side chain tpy-Ru(II)-tpy dicomplexes. Their characterization through TGA, UV-Vis, and Raman techniques revealed various modification degrees depending on the methodology employed. © 2009 Wiley Periodicals, Inc. J Polym Sci Part A: Polym Chem 47: 2551–2559, 2009
Keywords: carbon nanotubes; dendrimers; functionalization; metal-polymer complexes; Raman spectroscopy

INTRODUCTION

The combination of metal ions with polymers, semiconducting species, and furthermore with carbon nanotubes is a promising route for nanostructured composite materials with properties required in many modern, highly demanding technological applications.[1] Metal-ligand coordination bonding, especially bi- and ter-pyridine transition metal complexes, has been extended into a particularly useful tool toward supramolecular structures. Development of dendrimers and dendronized polymers, coordination, block, and star-like polymers are some of the areas' achievements, providing materials with enhanced catalytic, electrochemical, optical, and magnetic properties.[2]

Carbon nanotubes (CNTs),[3] single (SWCNTs) or multi (MWCNTs) walled have attracted academic and industrial interest due to their extraordinary mechanical, electrical, and thermal properties.[4] Their surface modification to increase their dissolution and processability properties has been the top priority of material scientists during the past decade. Several methodologies have been reported using covalent or noncovalent modifications of CNTs with polymers, organic, inorganic, or biological molecules.[5] The CNTs' noncovalent functionalization is mainly based on supramolecular complexation using various adsorption forces like van der Waals' and π-stacking interactions, or through polymer wrapping around the CNT, without risking the disruption of their extended

Correspondence to: A. K. Andreopoulou (E-mail: kandreop@chemistry.upatras.gr) or J. K. Kallitsis (E-mail: j.kallitsis@chemistry.upatras.gr)

Journal of Polymer Science: Part A: Polymer Chemistry, Vol. 47, 2551–2559 (2009)

π-network.[6] On the other hand, covalent[7] functionalization of CNTs using addition chemistry has also been developed either through the "grafting to" or the "grafting from" approaches. Among the various modifications exploited, dendron decoration of CNTs was initially attempted by Hirsch[8(a,b)] and Sun[8(c)] using mostly carboxylic acid functionalized CNTs, whereas direct attachment or development of dendrons onto the CNTs' surface have also been reported by the Prato group.[8(d)]

Herein, both the "grafting to" and "grafting from" routes were utilized for the functionalization of CNTs with terpyridine-Ru(II)-terpyridine moieties (tpy-Ru(II)-tpy). Dendritic terpyridines of the first generation (G1) bearing mono- or dialkoxy groups were employed to assure processability of the final hybrid CNT-metallocomplexes. Additionally, the CNTs utilized were either SWCNTs or MWCNTs. SWCNTs exhibiting simpler and more controllable structures have been preferred during laboratory research. However, MWCNTs are cheaper and produced in larger quantities, whereas maintaining most of the desired properties found in SWCNTs. Therefore, it is important to develop efficient and precise methodologies for their modification if such hybrid-CNTs are to be scaled up or commercialized.

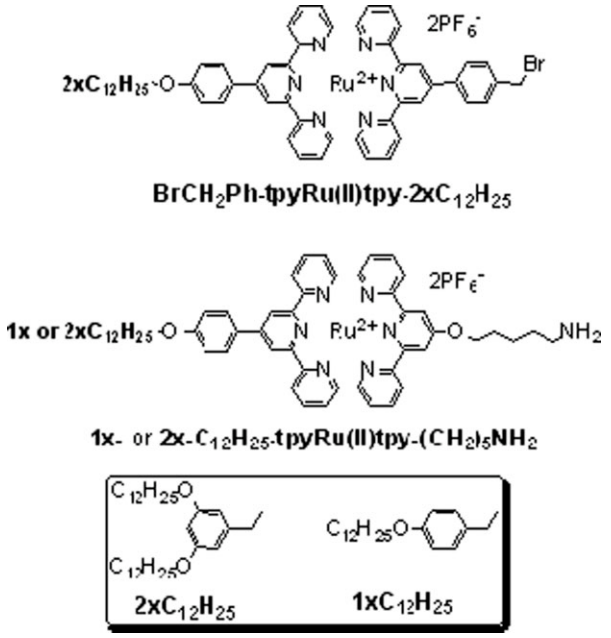

Scheme 1. Alkoxy tpy-Ru-(II)-tpy bromomethyl and amino functionalized complexes.

RESULTS AND DISCUSSION

Following the "grafting to" and "grafting from" approaches, three types of CNTs-tpyRu(II)tpy composites were prepared in this study. The bromomethyl terminated monomeric tpyRu(II)tpy complex (**$BrCH_2Ph$-tpyRu(II)tpy-2x$C_{12}H_{25}$**) of Scheme 1 was directly attached onto SWCNTs [Scheme 2(a)] using atom transfer radical addition conditions (ATRA).[9] On the other hand, the amino terminated complexes (**1x-** or **2x-$C_{12}H_{25}$-tpyRu(II)tpy-$(CH_2)_5NH_2$**, Scheme 1) were attached onto MWCNTs through solvent-free diazonium chemistry [Scheme 2(c)].[10] Moreover, side chain polymeric tpyRu(II)tpy complexes were developed onto SWCNTs employing ATR-polymerization[11] and subsequent metal complexation [Scheme 2(b)].

SWCNTs' functionalization with monomeric dendritic tpy-Ru(II)-tpy complexes bearing didodecyloxy groups using the "grafting to" approach is presented in Scheme 2(a). Metal-mediated atom transfer radical generation/addition (ATRA)[9] of complex **$BrCH_2Ph$-tpyRu(II)tpy-2x$C_{12}H_{25}$** (Scheme 1) onto the SWCNTs surface was accomplished using CuBr/PMDETA as the catalytic system. This catalytic system is also commonly used in ATRP reactions. Based on the thermogravimetric analysis (TGA) results (Fig. 1), the **SWCNT-tpyRu(II)tpy-2x$C_{12}H_{25}$** presented a 28.5% weight loss corresponding to 1 functional group per 400 carbon atoms.

Using the "grafting from" approach, SWCNTs were decorated with polymeric side chain dendritic tpy-Ru(II)-tpy complexes [Scheme 2(b)]. Initially, the reaction of pristine **SWCNTs** with 2-aminoethanol in DMF produced the **SWCNT-precursor** that was afterwards converted to the **SWCNT-initiator**.[12] The functional sites of **SWCNT-initiator** were used for the ATRP polymerization of the **vinyl-tpy**[13(a)] monomer producing **SWCNT-Poly(tpy)**. Even though, the polymerization was performed using CuBr/PMDETA in DMF at 110 °C, which is typical for ATRP; it is likely that the disproportionation step is very significant thus creating Cu^o species that act as catalyst under SET-LRP conditions (single electron transfer living radical polymerization).[14] For that reason, it is possible that both polymerization cycles (ATRP and SET-LRP) are present during the preparation of **SWCNT-Poly(tpy)** either in competitive or in cooperation modes. The free side-terpyridine groups of **SWCNT-Poly(tpy)**

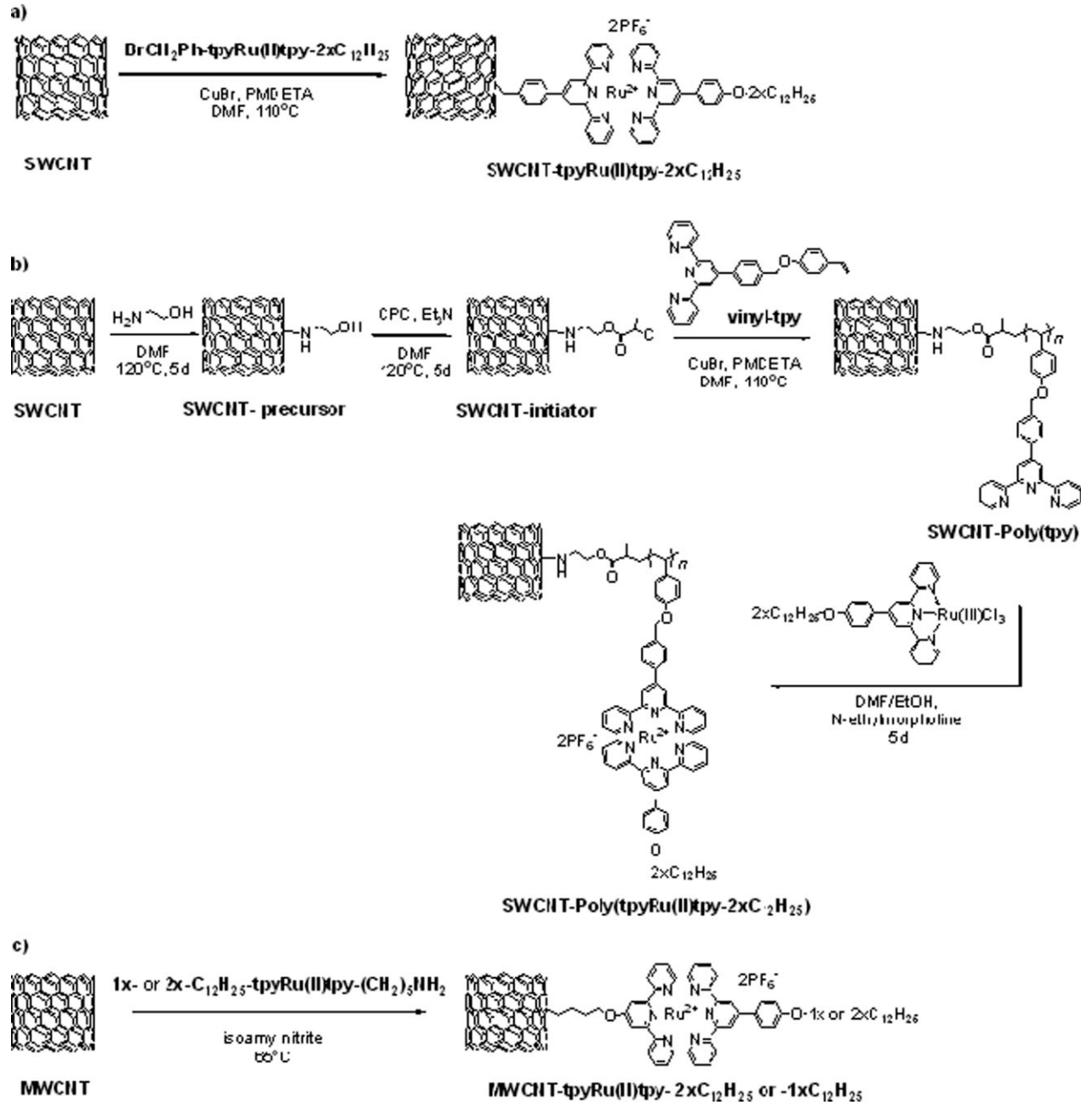

Scheme 2. Alkoxy tpy-Ru(II)-tpy functionalized CNTs.

were then complexated with the didodecyloxy-tpy-Ru(III)Cl_3 monocomplex (II)[13] affording the final hybrid nanotube-metallopolymeric complex **SWCNT-Poly(tpyRu(II)tpy-2x$C_{12}H_{25}$)**. Based on the TGA results of Figure 1, at 800 °C the pristine **SWCNT** presents a 9.5% weight loss and the SWCNT-precursor an additional 7.9% weight loss. Assuming that all the hydroxyl groups of **SWCNT-precursor** had reacted with 2-chloropropionyl chloride, a total weight loss of 27.6% at 800 °C would be expected. The actual **SWCNT-initiator**'s weight loss of 26.5% indicates that a 94.4% conversion of hydroxyl to ATRP initiator sites was achieved. The final **SWCNT-Poly(tpyRu(II)tpy-2x$C_{12}H_{25}$)** presented a 20.9% weight loss compared with the **SWCNT-initiator**. Its total weight loss compared with the pristine **SWCNT** at 800 °C was found to be 47.4%. Comparing the polymeric functionalized **SWCNT-Poly(tpyRu(II)tpy-2x$C_{12}H_{25}$)** with

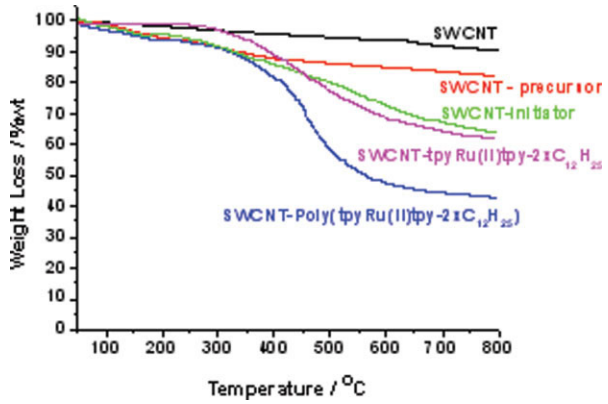

Figure 1. TGA thermograms of pristine and modified **SWCNTs** of Scheme 2(a,b).

the monomeric one, **SWCNT-tpyRu(II)tpy-2xC$_{12}$H$_{25}$**, we can observe the same decomposition stages, with the main weight loss obtained between 300 °C and 550 °C. Thus, we can conclude that a considerable Ru(II) loading was achieved also for the metallopolymer modified SWCNT.

On the other hand, MWCNTs having dendritic tpy-Ru(II)-tpy complexes with one or two dodecyloxy groups were prepared directly from the aminopentyl[15] functionalized dicomplexes **1x-** or **2x-C$_{12}$H$_{25}$-tpyRu(II)tpy-(CH$_2$)$_5$NH$_2$** (Scheme 1) using isoamyl nitrite, Scheme 2(c).[10] Representative TGA thermograms of the **MWCNT-tpyRu-(II)tpy-2xC$_{12}$H$_{25}$** and **1xC$_{12}$H$_{25}$** are given in Figure 2. The same transitions were observed for the **2x-C$_{12}$H$_{25}$-tpyRu(II)tpy-(CH$_2$)$_5$NH$_2$** and the **MWCNT-tpyRu(II)tpy-1x** or **2xC$_{12}$H$_{25}$** samples

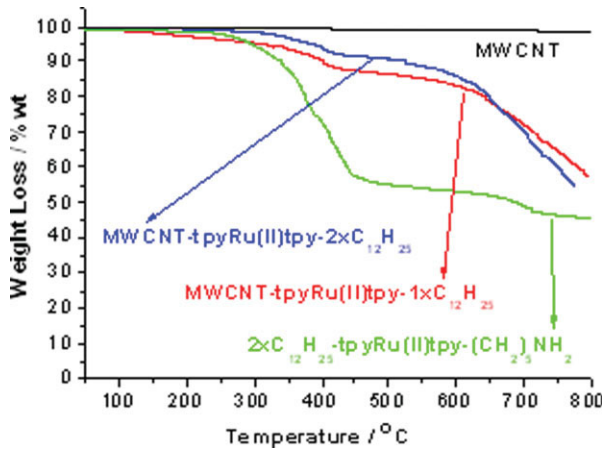

Figure 2. TGA thermogramms of **MWCNT-tpy-Ru(II)tpy-2xC$_{12}$H$_{25}$** and **1xC$_{12}$H$_{25}$**.

at 450 °C and ~650 °C. Since the TGA diagrams of the functionalized MWCNTs didn't reach a plateau up to 800 °C, we can only get an estimation of their weight loss at 500 °C that equals to 8.7% for **MWCNT-tpyRu(II)tpy-2xC$_{12}$H$_{25}$** and 12.7% for **MWCNT-tpyRu(II)tpy-1xC$_{12}$H$_{25}$**. Thus, a higher-degree of functionalization was accomplished for the **MWCNT-tpyRu(II)tpy-1xC$_{12}$H$_{25}$**.

All hybrid CNT-metallocomplexes prepared in this study were easily dispersible in organic solvents like DMF, THF, or DMSO, allowing characterization of their optoelectronic properties in solution. The UV-Vis examination in DMF solutions of the functionalized SWCNTs [Fig. 3(a)] and

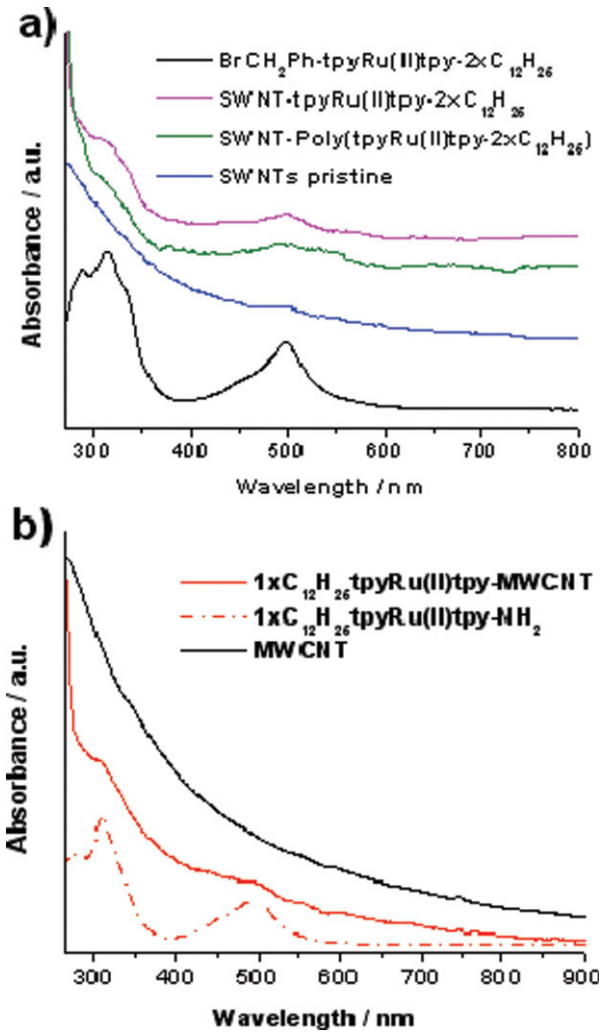

Figure 3. (**a**) UV-Vis spectra in DMF solutions of **SWCNT-tpyRu(II)tpy-2xC$_{12}$H$_{25}$** and **SWCNT-Poly(tpyRu(II)tpy-2xC$_{12}$H$_{25}$)** (**b**) UV-Vis in DMF solutions of **MWCNT-tpyRu(II)tpy-2xC$_{12}$H$_{25}$** and **-1xC$_{12}$H$_{25}$**.

MWCNTs [Fig. 3(b)] showed typical absorption bands corresponding to the MLCT (metal to ligand charge transfer) of the tpy-Ru(II)-tpy moieties at ~495 nm as well as the π-π^* transitions of the terpyridine ligands at ~310 nm. The UV-Vis spectra of the SWCNT-Ru(II) complexes were recorded only up to 800 nm since for the "NANOCYL" SWCNTs optical transitions between the van Hove singularities can be hardly observed.

Raman spectroscopy is a valuable tool used to characterize the functionalization of CNTs.[16] The Raman spectra of pristine **SWCNT**, **SWCNT-Poly(tpyRu(II)tpy-2xC$_{12}$H$_{25}$)**, and **SWCNT-tpyRu(II)tpy-2xC$_{12}$H$_{25}$**, excited with the 632.8 nm laser line, are presented in Figure 4(a). For pristine **SWCNTs**, the G band is comprised mainly of two peaks located at 1592 cm^{-1} and 1554 cm^{-1}, whereas the D band appears at 1321 cm^{-1}. The G-band originates from in-plane tangential stretching of the C—C bonds in graphene sheets. The D and D′ bands are disorder activated modes. It is well-documented that sidewall functionalization breaks the translational symmetry along the tube axis causing those modes to become Raman active. Therefore, an increase of the D-band intensity comprises a fingerprint for successful sidewall functionalization. Upon functionalization, an increase of the D-band intensity relative to the G one is clearly observed. By integrating the areas of the D and G peaks in Figure 4(a), the intensity ratio $(I(G^+)+I(G^-))/I(D)$ is ~5.4 for the pristine material while it reduces to ~3.0 and ~2.4 for **SWCNT-tpyRu(II)tpy-2xC$_{12}$H$_{25}$** and **SWCNT-Poly(tpyRu(II)tpy-2xC$_{12}$H$_{25}$)**, respectively. Also, it should be noted that a small contribution to the collected Raman scattering intensity of the **SWCNT-Poly(tpyRu(II)tpy-2xC$_{12}$H$_{25}$)** material from the polymeric chains cannot be discarded.

Figure 4(b) depicts the radial breathing modes (RBMs) for the pristine and modified samples using the 632.8 nm excitation wavelength. The frequency positions of the main peaks obtained with Lorentzian lineshapes are also shown. As it is apparent from Figure 4(b) significant changes of the Raman excitation profiles takes place in this part of the spectra most probably as a result of alterations in the resonance conditions of the hybrid materials due to covalent functionalization. Furthermore, the peaks located at 193 and 218 cm^{-1} for the pristine sample shift to 198 and 220 cm^{-1} for the **SWCNT-Poly(tpyRu(II)tpy-2xC$_{12}$H$_{25}$)**, respectively. The observed hardening

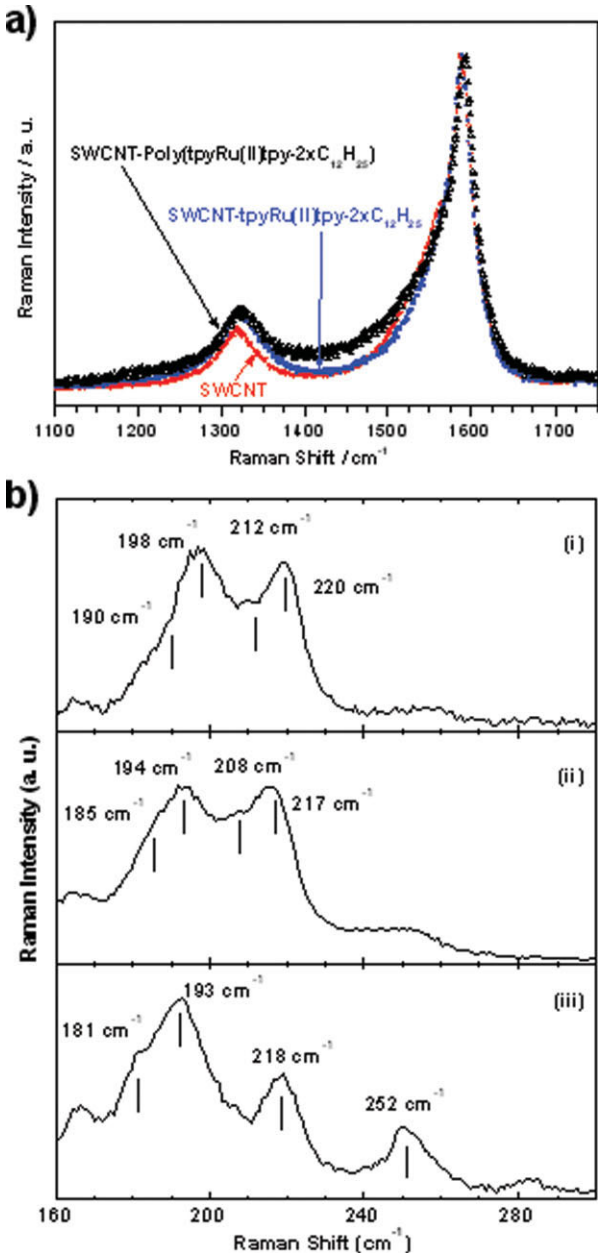

Figure 4. (**a**) Raman spectra for **SWCNTs** in the tangential mode frequency region and (**b**) Radial Breathing Modes (RBMs) for (i) **SWCNT-Poly(tpyRu(II)tpy-2xC$_{12}$H$_{25}$)**, (ii) **SWCNT-tpyRu(II)tpy-2xC$_{12}$H$_{25}$**, and (iii) pristine **SWCNT**. The vertical lines mark the main peaks of the studied materials. [Color figure can be viewed in the online issue, which is available at www.interscience.wiley.com.]

of the modes indicates that the decoration of SWCNTs with the polymeric chains affects considerably the force constant strength of the C—C bonds. Finally, for the **SWCNT-tpyRu(II)tpy-2xC$_{12}$H$_{25}$** hybrid minor frequency shifts can be

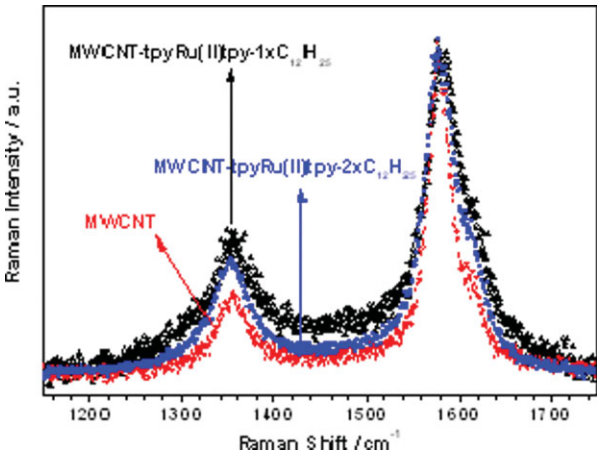

Figure 5. Raman spectra in the tangential mode frequency region of pristine **MWCNTs** and of **MWCNT-tpyRu(II)tpy-2xC$_{12}$H$_{25}$** and **1xC$_{12}$H$_{25}$**. [Color figure can be viewed in the online issue, which is available at www.interscience.wiley.com.]

observed in the Raman spectrum suggesting less pronounced interactions between SWCNTs and the functional groups.

The Raman spectra of pristine **MWCNT**, **MWCNT-tpyRu(II)tpy-2xC$_{12}$H$_{25}$**, and **MWCNT-tpyRu(II)tpy-1xC$_{12}$H$_{25}$** excited with the 514.5 nm laser line are shown in Figure 5. For the pristine material, three characteristic bands, namely the D-band at 1348 cm^{-1}, the G-band at 1580 cm^{-1}, and the D′-band at 1611 cm^{-1} have been detected. By integrating the areas of the D and G peaks for both samples, the G- to D- peak intensity ratio (IG/ID) for **MWCNT-tpyRu(II)tpy-1xC$_{12}$H$_{25}$** and **MWCNT-tpyRu(II)tpy-2xC$_{12}$H$_{25}$** are ~1.6 and ~2.1, respectively. For pristine MWCNTs, a considerable enhancement of the corresponding ratio IG/ID (~2.8) is estimated. Those findings further support the disruption of the graphitic integrity due to the proposed covalent functionalization. Also, the D′ which can be barely observed in pristine tubes as a shoulder at 1615 cm^{-1} is clearly detectable after functionalization, reflecting an enhancement of the tubes structural disorder caused by sp^3 hybridization of the sidewall carbon atoms. Additionally, it should be stressed that for the **MWCNT-tpyRu(II)tpy-1xC$_{12}$H$_{25}$** sample a blue shift of ~3 cm^{-1} was found for the G band relative to the pristine one, whereas a negligible shift is observed for the **MWCNT-tpyRu(II)tpy-2xC$_{12}$H$_{25}$** compound. Moreover, the full-width at half maximum (FWHM) of the G-band is significantly affected upon functionalization. The FWHM for the pristine material is 29 cm^{-1} and increases significantly to 49 cm^{-1} for 1xC$_{12}$H$_{25}$- and to 39 cm^{-1} for **MWCNT-tpyRu(II)tpy-2xC$_{12}$H$_{25}$**. These results show that a more efficient functionalization was achieved in the case of **MWCNT-tpyRu(II)tpy-1xC$_{12}$H$_{25}$** in agreement with the results obtained from TGA.

It is evident that using the above methodologies, we succeeded in decorating various types of CNTs with terpyridine-ruthenium complexes, combining the complexes' properties with those arising from CNTs. For solubility reasons of the CNT-metallomonomers and CNT-metallopolymers used herein, long aliphatic chains were attached on the terpyridines which effectively acted as solubilizers of the final hybrid metallo-CNTs. As it is well-known, such long aliphatic substituents located on the outer sphere of dendrimers and dendronized polymers lead to enhanced organizational features.[17] Certainly, such self-organization phenomena are not expected for the functionalized CNTs of this study, due to the inherent and predominant, long and rigid nature of the central graphene core. However, the solubility enhancement that these substituents bring to the system is of significant importance for the creation of prossessable CNT based nanomaterials.

CONCLUSIONS

It has been demonstrated that CNTs can be efficiently functionalized with terpyridine-Ru(II)-terpyridine complexes either as monomeric dicomplexes or as polymeric chains bearing side tpy-Ru(II)tpy moieties onto every repeating unit. The employment of both pristine SWCNTs and MWCNTs in combination with the efficiency of either the "grafting to" or "grafting from" approaches reveals the effectiveness and tolerance of the above functionalizations toward processable hybrid metallocontaining CNTs. All characterization techniques employed proved the herein poröse CNTs modifications. This methodology enables the CNTs' functionalization in desirable degrees and can be extended in the attachment of other complexes and different metal ions as well.

EXPERIMENTAL

Materials

The SWNTs used in this work were obtained from NANOCYL S.A. (SWCNT 90+% C purity) and the

MWCNTs from "NANOTHINX S.A." 4-(2,2′:6′,2″-terpyridin-4′-yl)benzyl bromide,[18] didodecyloxy- and mono-dodecyloxy-terpyridine/ruthenium(III) trichloride mono-complexes,[13(a)] **vinyl-tpy**,[13(a)] 5-aminopentyl 4′-(2,2′:6′,2″-terpyrydinyl)ether[15] and **SWCNT-initiator**[12(f)] were synthesized according to literature procedures. CuBr (Aldrich), 2,2′-bipyridine (bipy, Aldrich), *N,N,N′,N′,N″*-pentamethyldiethylene triamine (PMDETA, Aldrich) and all the other reagents and solvents were used as received. All the polymerization and complexation reactions were carried out under an argon atmosphere.

Instrumentation

The structures of the synthesized monomeric compounds were clarified by high-resolution ^{1}H and ^{13}C NMR spectroscopies with Bruker Advance DPX 400 MHz and 100 MHz spectrometers, respectively. UV-Vis spectra were recorded using a Hitatchi spectrophotometer model U 1800 in quartz glass cuvettes (1 cm). The TGA experiments were performed on a TA Instruments Q50 series. Raman spectra of MWCNT and SWCNT samples were recorded using a microscope equipped triple monochromator combined with a Peltier cooled charge-coupled device detector system. The spectra were acquired in the back-scattering geometry using the 514.5 nm and the 632.8 nm excitation lines. The light was focused on the samples using an 80× objective. The data were recorded at the laser power of 0.4 mW, measured directly before the samples, to minimize heating effects. The phonon frequencies were obtained by fitting Lorentzian lineshapes to the experimental peaks.

$BrCh_2Ph$-tpyRu(II)tpy-2x$C_{12}H_{25}$

A round bottom flask equipped with a reflux condenser a magnetic stirrer and a gas inlet/outlet was flamed under vacuum. 50 mg (0.124 mmol) of 4-(2,2′:6′,2″-terpyridine-4′-yl)benzyl bromide and 184 mg (0.186 mmol) of didodecyloxy-terpyridine/ruthenium(III)trichloride monocomplex were mixed in 30 mL of a 4:1 mixture of THF and EtOH. Five drops of *N*-ethylmorpholine were added, and the mixture was heated to reflux for 2 days. After the removal of insoluble byproducts by filtration through Celite, the resulting deep red filtrate was evaporated to almost half its volume. The addition of an excess of a saturated NH_4PF_6/MeOH solution caused the complex to precipitate as a dark-red powder, which was filtered and washed with EtOH, H_2O, and toluene. The desired dicomplex **$BrCH_2Ph$-tpyRu(II)tpy-2x$C_{12}H_{25}$** (120 mg, 69%) was obtained by reprecipitation from $CHCl_3$ (10 mL) into *n*-hexane (100 mL) and then dried under vacuum at 40 °C. δ_H (400 MHz; DMSO-d6; Me4Si): 0.86 (CH_3, s, 6H), 1.27–1.40 (CH_2, s, 32H), 1.45 (CH_2, s, 4H), 1.74 (CH_2, s, 4H), 4.00 (OCH_2, s, 4H), 4.97 (CH_2-Br, s, 2H), 5.26 (OCH_2, s, 2H), 6.47 ($C_{Ar}H$, s, 1H), 6.68 ($C_{Ar}H$, s, 2H), 7.28 ($C_{Ar}H$, d, 4H), 7.40 ($C_{Ar}H$, d, 4H), 7.52 ($C_{Ar}H$, s, 4H), 8.00 ($C_{Ar}H$, s, 4H), 8.41 ($C_{Ar}H$, m, 4H), 9.04 ($C_{Ar}H$, s, 4H), 9.42 ppm($C_{Ar}H$, s, 4H).

Synthesis of SWCNT-tpyRu(II)tpy-2x$C_{12}H_{25}$

A round-bottom flask equipped with a rubber septum, a magnetic stirrer, and a gas inlet/outlet was flamed under vacuum. 11 mg (0.077 mmol) of CuBr and 160 μL (0.077 mmol) of *N,N,N′,N″,N″*-pentamethyldiethylenetriamine (PMDETA) were added along with 25 mg of SWCNTs. The system was degassed and flushed with argon again. The solvent DMF (degassed) 3 mL and 100 mg (0077 mmol) of **$BrCH_2Ph$-tpyRu(II)tpy-2x$C_{12}H_{25}$** were added to the flask and the reaction mixture was immediately degassed and flushed with argon. The reaction mixture was then immersed in an oil bath and heated at 110 °C for 24 h. After cooling to room temperature, the suspension was filtered through a Millipore PTFE 0.2 μm membrane and consecutively washed with $CHCl_3$, THF, Acetone, and DMF to remove any unreacted materials. The solid remaining onto the membrane was dispersed in DMF with an ultrasonic bath and consecutively filtered through a PTFE 0.2-μm membrane. The procedure was repeated three times. The CNTs were finally filtered, washed with Acetone and Diethyl Ether and then dried under vacuum at 50 °C overnight.

Synthesis of SWCNT-Poly(tpyRu(II)tpy-2x$C_{12}H_{25}$)

SWCNT-Poly(tpy)

The same system/procedure as for **SWCNT-tpyRu(II)tpy-2x$C_{12}H_{25}$** was followed using the modified **SWCNT-initiator** (25 mg, 0.946 μmol of initiator sites), 82 mg (0.19 mmol) of **vinyl-tpy**, 5.5 mg (0.038 mmol) of CuBr, 8 μL (0.038 mmol) of PMDETA, and 3 mL of degassed DMF. The **SWCNT-Poly(tpy)** were equally treated as before to remove impurities and excess of reagents.

SWCNT-Poly(tpyRu(II)tpy-2xC$_{12}$H$_{25}$). A round bottom flask, equipped with a reflux condenser a magnetic stirrer and a gas inlet/outlet was flamed under vacuum. The modified **SWCNT-Poly(tpy)** were added to the flask along with a double excess in molar ratio of the didodecyloxy-terpyridine/ruthenium(III) trichloride monocomplex (compared with the terpyridine amount formerly used), a 30 mL mixture of THF/EtOH 4/1 and five drops of *N*-ethylmorpholine. The reaction mixture was refluxed at 70 °C for 5 days. Then the suspension was filtered through a Millipore PTFE 0.2 μm membrane and consecutively washed with $CHCl_3$, THF, Acetone, and DMF to remove any unreacted materials. The solid remaining onto the membrane was treated with ultrasonic bath in DMF and consecutively filtered through a PTFE 0.2-μm membrane. The procedure was repeated three times. The **SWCNT-Poly(tpyRu(II)tpy-2xC$_{12}$H$_{25}$)** was finally filtered and washed with Acetone and Diethyl Ether and then dried under vacuum at 50 °C overnight.

1x- or 2x-C$_{12}$H$_{25}$-tpyRu(II)tpy-(CH$_2$)$_5$NH$_2$

General procedure for the synthesis of **1x-** or **2x-C$_{12}$H$_{25}$-tpyRu(II)tpy-(CH$_2$)$_5$NH$_2$** complexes as follows: The didodecyloxy- or mono-dodecyloxy-terpyridine/ruthenium(III) trichloride monocomplexes (1.02 mmol) and 5-aminopentyl 4′-(2,2′:6′,2″-terpyrydinyl)ether (1.00 mmol) were mixed in 30 mL of a 2:1 mixture of THF/EtOH. Five drops of *N*-ethylmorpholine were added and the mixture was heated to reflux for 2 days. After removing insoluble byproducts by filtration through celite, the resulting deep red filtrate was evaporated to almost half its volume. Addition of excess of a saturated NH_4PF_6/MeOH/H_2O solution caused the complex to precipitate as a red powder, which was filtrated and washed with EtOH, H_2O and *n*-hexane.

2x-C$_{12}$H$_{25}$-tpyRu(II)tpy-(CH$_2$)$_5$NH$_2$ Yield 85%. δ_H (400 MHz; DMSO-d6; Me4Si): 9.37 (s, 2H, ArH), 9.04 (d, 2H, ArH), 8.84 (d, 2H, ArH), 8.75 (s, 2H, ArH), 8.38 (d, 2H, ArH), 7.97–8.03 (m, 4H, ArH), 7.2–7.5 (m, 10H, ArH), 6.4 (s, 2H, ArH), 6.44 (s, 1H, ArH), 5.22 (s, 2H, $ArCH_2O$), 4.55 (t, 2H, CH_2), 3.95 (t, 4H, OCH_2), 2.87 (m, 2H, CH_2), 1.9 (m, 4H, CH_2, NH_2), 1.67 (m, 8H, CH_2), 1.1–1.4 (m, 36H, CH_2), 0.8 (t, 6H, CH_3).

1x-C$_{12}$H$_{25}$-tpyRu(II)tpy-(CH$_2$)$_5$NH$_2$ Yield 80%. δ_H (400 MHz; DMSO-d6; Me4Si): 9.4 (s, 2H, ArH), 9.1 (s, 2H, ArH), 8.78–8.88 (m, 4H, ArH), 8.43 (d, 2H, ArH), 8.06 (m, 4H, ArH), 7.2–7.55 (two m, 10H, ArH), 4.54 (t, 2H, CH_2), 4.16 (t, 2H, OCH_2), 2.9 (m, 2H, CH_2), 1.92 (m, 4H, CH_2, NH_2), 1.6 (m, 6H, CH_2), 1.2–1.5 (m, 18H, CH_2), 0.87 (t, 3H, CH_3).

Synthesis of MWCNT-tpyRu(II)tpy-2xC$_{12}$H$_{25}$ or -1xC$_{12}$H$_{25}$

To a degassed flask equipped with a reflux condenser and a gas inlet/outlet, 50 mg of MWCNTs (Nanothinx S.A.), 50 mg (0.041 mmol) of **1xC$_{12}$H$_{25}$-tpyRu(II)tpy-(CH$_2$)$_5$NH$_2$** or 50 mg (0.0331 mmol) of **2xC$_{12}$H$_{25}$-tpyRu(II)tpy-(CH$_2$)$_5$NH$_2$**, and 1 mL (7.44 mmol) of isoamyl nitrite were added under argon atmosphere and in absence of light. The reaction mixture was degassed and flushed with argon again and refluxed at 65 °C for 5 days. Then, it was left to cool down to room temperature and filtered through a Millipore PTFE 0.2-μm membrane. The **MWCNT-tpyRu(II)tpy-2xC$_{12}$H$_{25}$** or **-1xC$_{12}$H$_{25}$** remaining onto the membrane were washed with excess of Acetone, followed by ultrasonic bath in DMF and consecutively filtered again through a PTFE 0.2-μm membrane. The procedure was repeated three times to remove any excess of unreacted materials. The functionalized MWCNTs were finally filtered, washed with Acetone and Diethyl Ether, and then dried under vacuum at 50 °C overnight.

The authors gratefully acknowledge "Nanothinx S.A." Rio Patras, Greece, for the MWCNTs used in this study. This project was partially supported from the Greek Ministry of Development under the research grant PENED 03ED118 "Organic Solar Cells" cofinanced by E.U.-European Social Fund (75%) and the Greek Ministry of Development-GSRT (25%); and from the European Commission through the European program APOLLON B, NMP3 CT-2006-033228 (2006–2009).

REFERENCES AND NOTES

1. (a) Tasis, D.; Tagmatarchis, N.; Bianco, A.; Prato, M. Chem Rev 2006, 106, 1105–1136; (b) Rotas, G.; Sandanayaka, A. S. D.; Tagmatarchis, N.; Ichihashi, T.; Yudadaka, M.; Iijima, S.; Ito, O. J Am Chem Soc 2008, 130, 4725–4731.
2. (a) Schubert, U. S.; Eschbaumer, C. Angew Chem Int Ed 2002, 41, 2892–2926; (b) Lohmeijer, B. G. G.; Schubert, U. S. Angew Chem Int Ed 2002, 41, 3825–3829; (c) Shunmugam, R.; Tew, G. N. J Am Chem Soc 2005, 127, 13567–13572; (d) Aamer, K.

A.; De Jeu, W. H.; Tew, G. N. Macromolecules 2008, 41, 2022–2029.
3. (a) Iijima, S. Nature 1991, 354, 56–58; (b) Iijima, S.; Ichihashi, T. Nature 1993, 363, 603–605.
4. (a) Dresselhaus, M. S.; Dresselhaus, G.; Avouris, P. In Carbon Nanotubes: Synthesis Structure, Properties, and Applications; Springer: Berlin, 2001; (b) Ajayan, P. M. Chem Rev 1999, 99, 1787–1800; (c) Saito, R.; Dresselhaus, G.; Dresselhaus, M. S. In Physical Properties of Carbon Nanotubes; Imperial College Press: London, 1998.
5. Hirsch, A.; Vostrowsky, O. Top Curr Chem 2005, 245, 193–237.
6. (a) Chen, R. J.; Zhang, Y.; Wang, D.; Dai, H. J Am Chem Soc 2001, 123, 3838–3839; (b) Yang, L. P.; Pan, C. Y. Macromol Chem Phys 2008, 209, 783–793; (c) Petrov, P.; Stassin, F.; Pagnoulle, C.; Je'rome, R. Chem Commun 2003, 2904–2905; (d) Chen, J.; Liu, H. Y.; Weimer, W. A.; Halls, M. D.; Waldeck, D. H.; Walker, G. C. J Am Chem Soc 2002, 124, 9034–9035; (e) Steuerman, D. W.; Star, A.; Narizzano, R.; Choi, H.; Ries, R. S.; Nicolini, C.; Stoddart, J. F.; Heath, J. R. J Phys Chem B 2002, 106, 3124–3130; (f) Star, A.; Liu, Y.; Grant, K.; Ridvan, L.; Stoddart, J. F.; Steuerman, D. W.; Diehl, M. R.; Boukai, A.; Heath, J. R. Macromolecules 2003, 36, 553–560; (g) Ou, Y. Y.; Huang, M. H. J Phys Chem B 2006, 110, 2031–2036.
7. (a) Holzinger, M.; Vostrowsky, O.; Hirsch, A.; Hennrich, F.; Kappes, M.; Weiss, R.; Jellen, F. Angew Chem Int Ed 2001, 40, 4002–4005; (b) Bahr, J. L.; Yang, J.; Kosynkin, D. V.; Bronikowski, M. J.; Smalley, R. E.; Tour, J. M. J Am Chem Soc 2001, 123, 6536–6542; (c) Georgakilas, V.; Kordatos, K.; Prato, M.; Guldi, D. M.; Holzinger, M.; Hirsch, A. J Am Chem Soc 2002, 124, 760–761; (d) Tagmatarchis, N.; Prato, M. J Mater Chem 2004, 14, 437–439; (e) Mountrichas, G.; Pispas, S.; Tagmatarchis, N. Chem Eur J 2007, 13, 7595–7599; (f) Wu, W.; Tsarevsky, N. V.; Hudson, J. L.; Tour, J. M.; Matyjaszewski, K.; Kowalewski, T. Small 2007, 3, 1803–1810; (g) Georgakilas, V.; Bourlinos, A.; Gournis, D.; Tsoufis, T.; Trapalis, C.; Aurelio, M.-A.; Prato, M. J Am Chem Soc 2008, 130, 8733–8740.
8. (a) Holzinger, M.; Hirsch, A.; Bernier, P.; Duesberg, G. S.; Burghard, M. Appl Phys A 2000, 70, 599–602; (b) Holzinge, M.; Abraham, J.; Whelan, P.; Graupner, R.; Ley, L.; Hennrich, F.; Kappes, M.; Hirsch, A. J Am Chem Soc 2003, 125, 8566–8580; (c) Sun, Y. P.; Huang, W.; Lin, Y.; Fu, K.; Kitaygorodskiy, A.; Riddle, L. A.; Yu, Y. J.; Carroll, D. L. Chem Mater 2001, 13, 2864–2869; (d) Campidelli, S.; Sooambar, C.; Diz, E. L.; Ehli, C.; Guldi, D. M.; Prato, M. J Am Chem Soc 2006, 128, 12544–12552.
9. (a) Iqbal, J.; Bhatia, B.; Nayyar, N. K. Chem Rev 1994, 94, 519–564; (b) Stalmach, U.; De Boer, B.; Videlot, C.; van Hutten, P. F.; Hadziioannou, G. J Am Chem Soc 2000, 122, 5464–5472; (c) Homenick, C. M.; Lawson, G.; Adronov, A. Polym Rev 2007, 47, 265–290; (d) Pintauer, T.; Matyjaszewski, K. Chem Soc Rev 2008, 37, 1087–1097.
10. (a) Christopher, A. D.; Tour, J. M. J Am Chem Soc 2003, 125, 1156–1157; (b) Friedman, L.; Bayless, H. J. J Am Chem Soc 1969, 91, 1790–1794.
11. (a) Matyjaszewski, K. Chem Eur J 1999, 5, 3095–3102; (b) Matyjaszewski, K.; Xia, J. Chem Rev 2001, 101, 2921–2990; (c) Kamigaito, M.; Ando, T.; Sawamoto, M. Chem Rev 2001, 101, 3689–3746.
12. (a) Baskaran, D.; Mays, W. J.; Bratcher, S. M. Angew Chem Int Ed 2004, 43, 2138–2142; (b) Qin, S.; Qin, D.; Ford, W. T.; Resasco, D. E.; Herrera, J. E. J Am Chem Soc 2004, 126, 170–176; (c) Kong, H.; Gao, C.; Yan, D. J Am Chem Soc 2004, 126, 412–413; (d) Kong, H.; Li, W.; Gao, C.; Yan, D.; Jin, Y.; Walton, D. R. M.; Kroto, H. W. Macromolecules 2004, 37, 6683–6686; (e) Kong, H.; Gao, C.; Yan, D. Macromolecules 2004, 37, 4022–4030; (f) Chochos, C. L.; Stefopoulos, A. A.; Campidelli, S.; Prato, M.; Gregoriou, V. G.; Kallitsis, J. K. Macromolecules 2008, 41, 1825–1830; (g) Stefopoulos, A. A.; Chochos, C. L.; Prato, M.; Pistolis, G.; Papagelis, K.; Petraki, F.; Kennou, S.; Kallitsis, J. K. Chem Eur J 2008, 14, 8715–8724.
13. (a) Tzanetos, N. P.; Andreopoulou, A. K.; Kallitsis, J. K. J Polym Sci Part A: Polym Chem 2005, 43, 4838–4848; (b) Andreopoulou, A. K.; Kallitsis, J. K. Eur J Org Chem 2005, 4448–4458.
14. (a) Percec, V.; Guliashvili, T.; Ladislaw, J. S.; Wistrand, A.; Stjerndahl, A.; Sienkowska, M. J.; Monteiro, M. J.; Sahoo, S. J. Am Chem Soc 2006, 128, 14156–14165; (b) Guliashvili, T.; Percec, V. J Polym Sci Part A: Polym Chem 2007, 45, 1607–1618; (c) Rosen, B. M.; Percec, V. J Polym Sci Part A: Polym Chem 2008, 46, 5663–5697; (d) Lligadas, G.; Rosen, B. M.; Monteiro, M. J.; Percec, V. Macromolecules 2008, 41, 8360–8364.
15. Newkome, G. R.; He, E. J Mater Chem 1997, 7, 1237–1244.
16. Graupner, R. J Raman Spectrosc 2007, 38, 673–683.
17. (a) Schluter, A. D. Top Curr Chem 2005, 245, 151–191; (b) Percec, V.; Glodde, M.; Bera, T. K.; Miura, Y.; Shiyanovskaya, I.; Singer, K. D.; Balagurusamy, V. S. K.; Heiney, P. A.; Schnell, I.; Rapp, A.; Spiess, H.-W.; Hudson, S. D.; Duan, H. Nature 2002, 419, 384–387; (c) Percec, V.; Rudick, J. G.; Peterca, M.; Heiney, P. A. J Am Chem Soc 2008, 130, 7503–7508; (d) Percec, V.; Won, B. C.; Peterca, M.; Heiney, P. A. J Am Chem Soc 2007, 129, 11265–11278; (e) Andreopoulou, A. K.; Carbonnier, B.; Kallitsis, J. K.; Pakula, T.; Macromolecules 2004, 37, 3576– 3587.
18. Hanabusa, K.; Nakamura, A.; Koyama, T.; Shirai, H. Makromol Chem 1992, 193, 1309–1319.

End-Functionalization of Semiconducting Species with Dendronized Terpyridine–Ru(II)–Terpyridine Complexes

ELEFTERIOS K. PEFKIANAKIS,[1] NIKOLAOS P. TZANETOS,[1] CHRISTOS L. CHOCHOS,[1,2] AIKATERINI K. ANDREOPOULOU,[1] JOANNIS K. KALLITSIS[1,2]

[1]Department of Chemistry, University of Patras, GR-26504 Rio-Patras, Greece

[2]Foundation of Research and Technology Hellas, Institute of Chemical Engineering and High Temperature Processes, P.O. Box 1414, GR-26504 Rio-Patras, Greece

Received 2 October 2008; accepted 9 January 2009
DOI: 10.1002/pola.23289
Published online in Wiley InterScience (www.interscience.wiley.com).

ABSTRACT: Semiconducting oligomers and polymers decorated with two or one dendronized tpy-Ru(II)-tpy metallocomplexes are presented. Initially, free terpyridine end-functionalized semiconducting oligomers (distyrylanthracene, quinquephenylene, mono- and trifluorenes) were prepared while in a second approach, atom transfer radical polymerization was employed for the preparation of side-chain oligomeric and polymeric (oxadiazole)s using a terpyridine initiator. These terpyridine-bearing oligomers and polymers were complexated with a Percec-type first-generation (G1) dendronized terpyridine–Ru(III)Cl_3 monocomplex, having two dodecyloxy groups. All oligomeric and polymeric metallocomplexes were characterized via NMR spectroscopies for their structural perfection and via UV-Vis and PL spectroscopies for their optical properties. The existence of the organic semiconducting blocks in combination with the terpyridine–Ru(II)–terpyridine groups afforded hybrid metallo-semiconducting species presenting the optical features of both their components. Moreover, their thin-film morphologies were investigated through atomic force microscopy, revealing, in some cases, an organization tendency in the nanometer scale. © 2009 Wiley Periodicals, Inc. J Polym Sci Part A: Polym Chem 47: 1939–1952, 2009

Keywords: dendrimers; heteroatom-containing polymers; metal-polymer complexes; semiconducting oligomers; supramolecular structures

INTRODUCTION

Metal ions incorporated into typical carbon-based organic systems result in materials with redox, magnetic, optical, or reactive properties, not easily accessible otherwise. Metal complexes of the 2,2′-bipyridine (bpy) and 2,2′:6′,2′-terpyridine (tpy) ligands have proven most useful not only due to their complexation ability with different metal ions such as Ir, Rh, Os, Ru, Cu, Fe, Zn, Ni and so forth but also due to their ease of synthesis, and in various substitution patterns, thus, a great number of metal-bearing systems have been developed.[1] In recent years, they have been studied widely in solar energy conversion,[2] light-emitting electrochemical cells,[3] luminescent and electroluminescent materials,[4] nonlinear optical devices,[5] and organic light-emitting diodes.[6] In general, the optoelectronic properties of polypyridine–transition metal ion complexes can be tailored to create semiconducting multicomponent systems in combination with known fully organic semiconducting oligomeric or polymeric species.

Correspondence to: A. K. Andreopoulou (E-mail: kandreop@chemistry.upatras.gr)

Journal of Polymer Science: Part A: Polymer Chemistry, Vol. 47, 1939–1952 (2009)

Particularly, the stability and the ease of synthesis of Ru(II) complexes have favored intense research.[7–9] Ru(II) complexes based on bidentate bipyridine ligands have excellent photophysical properties.[10–12] However, these complexes are chiral whereas the tridentate terpyridine ones are achiral, offering stereochemical and purification advantages.[13–20] On the other hand, the main drawback of tpy–Ru(II)–tpy complexes is that they are practically nonluminescent at room temperature, which has triggered efforts toward the improvement of their optoelectronic properties.[21,22] Nonetheless, the possibilities that tpy–Ru(II)–tpy complexes offer for the formation of metal-based systems using metal–ligand coordinative bonding have led to a large number of self-assembled hybrid supramolecular systems. Thus, tpy–Ru(II)–tpy complexes have extensively been introduced into backbones,[23] side-chains,[24,25] as well as chain ends and centers[26–30] of (co)polymers; into the core, periphery, or branching points of dendrimers and dendronized polymers;[31–33] as well as various other symmetric or asymmetric architectures.[34] Additionally, the self-assembly of terpyridines under complexation with metal ions can produce discrete semiconducting hybrid oligomers with well-defined chemical structures and electronic properties.[35]

Taking the above into consideration, we prepared a series of semiconductingt *p*-conjugated oligomers end-functionalized with two free terpyridine moieties that were selectively complexated with a dendritic dialkoxy tpy–Ru(III) monocomplex[32] of the first generation (G1). Secondly, semiconducting oligomeric- and polymeric-(oxadiazole)s were synthesized under atom transfer radical polymerization (ATRP)[36] using a free terpyridine as the initiator, a method affording end-functionalized tpy–(oxadiazole)s that were also selectively complexated with the dendritic dialkoxy tpy–Ru(III) monocomplex. The didodecyloxy–tpy–Ru(III)Cl_3 monocomplexes were selected to assure the solubility for the final hybrid systems due to the long alkoxy groups and also to investigate the self-organizational ability of such dendritic moieties onto the metal-loaded materials. On the basis of previous findings of dendronized systems, such long aliphatic substituents located on the outer sphere of dendrimers and dendronized polymers lead to enhanced organizational features. Dendronization of rigid or flexible, macromolecular or oligomeric specimens has extensively been employed to induce the self-assembly to the final materials. Impressive helical, ribbon-like, columnar, or cylindrical architectures have been demonstrated due to the dendritic parts and also in combination with H-bonding, π–π stacking, and hydrophobic–hydrophilic interactions. Especially, self-assembled *p*-conjugated oligomeric entities are expected to influence the morphology and performance of optoelectronic and photovoltaic devices.[37–42] Thus, the dendritic tpy–Ru(II)–tpy-modified semiconducting materials presented herein were characterized with respect to their structural perfection, optoelectronic properties, and self-assembly in solid state.

EXPERIMENTAL

Materials

4′-(2,2′:6′,2″-Terpyridin-4′-yl)benzyl bromide (**I**),[43] compounds **R1**,[44] **R2**,[45] **R3**,[46] and **R4**[47] (Scheme 1), 2-[4-(4-vinylbenzyloxy)phenyl]-5-phenyl-1,3,4-oxadiazole (**vinyl-oxadiazole**)[44(a),44(b)] (Scheme 2) and didodecyloxy-terpyridine/ruthenium(III) mono-complex (**II**)[32] were synthesized as described in the literature. Diphenyl ether (Merck) was stored over molecular sieves (4 Å) and purged with argon for 30 min before the polymerization was started. CuBr (Aldrich), 2,2′-bipyridine (bpy, Aldrich), *N,N,N′,N′,N′*-pentamethyldiethylene triamine (PMDETA, Aldrich) and all the other reagents and solvents were used as received. All the polymerization and complexation reactions were carried out under argon atmosphere.

Instrumentation

The structures of the synthesized compounds were clarified by high-resolution ^{1}H and ^{13}C NMR spectroscopies with Bruker Avance DPX 400 MHz and 100 MHz spectrometers, respectively. Molecular weights (M_n and M_w) were determined by gel permeation chromatography [GPC; Ultrastyragel columns with 500 and 10^4 Å pore size; $CHCl_3$ (analytical grade) was filtered through a 0.5-μm Millipore filter and samples were passed through a 0.2-μm Millipore filter; flow 1 mL min^{-1}; at room temperature] using polystyrene standards for calibration. UV-Vis spectra were recorded using a Hitatchi spectrophotometer, model U 1800. All spectroscopic measurements were performed in quartz glass cuvettes (1 cm). Photoluminescence was measured using a Perkin–Elmer LS45 spectrofluorometer in $CHCl_3$ solutions of 10^{-6} M concentrations. Imaging of the surface

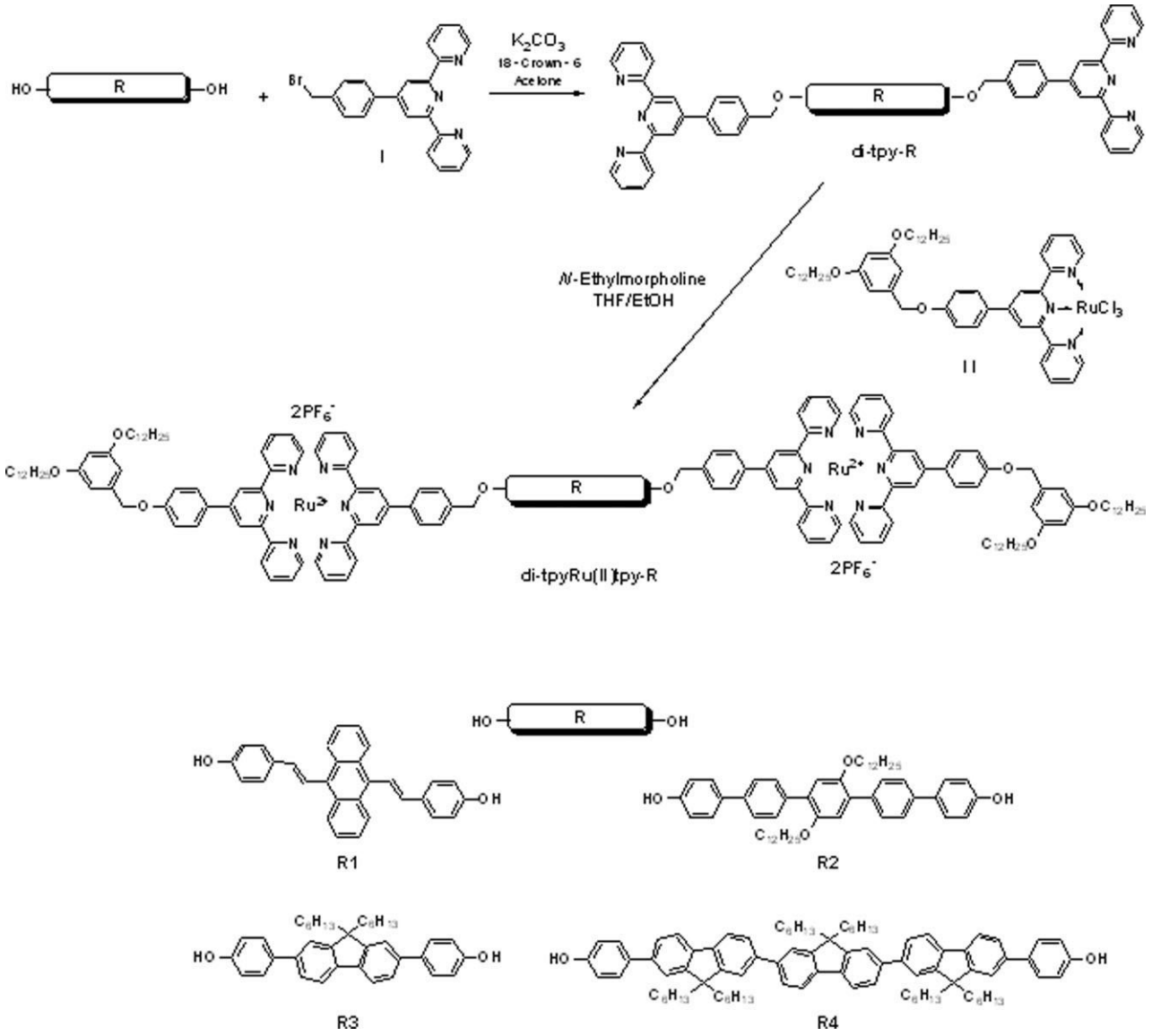

Scheme 1. Synthetic procedure for dendronized **ditpyRu(II)tpy-R** semiconducting oligomeric dicomplexes with **R1** = distyrylanthracene, **R2** = didodecyloxy-quinquephenyl, **R3** = fluorine, and **R4** = trifluorene segments.

morphology of the spin-coated samples was accomplished via atomic force microscopy (AFM), using a Topometrix Explorer SPM Microscope (Theromicroscopes) with Electronic control unit ECU-Plus TM and Explorer SPM head with Truemetrix Scan Linearization having two dry scanners.

General Procedure for the Synthesis of the Compounds *ditpy-R (R1–R4)*

A mixture of the compounds **R1–R4**, 4′-(2,2′:6′,2″-terpyridin-4′-yl)benzyl bromide (**I**), K_2CO_3, and 18-crown-6, in acetone (30 mL) was refluxed for 48 h under argon atmosphere. After cooling to room temperature, the resulting precipitate was filtered off, washed with water (3 × 10 mL), additional acetone (3 × 5 mL), and dried under vacuum at 40 °C.

Compound **ditpy-R1**: 0.100 g (0.242 mmol) of **R1**, 0.243 g (0.604 mmol) of **I**, 0.067 g (0.483 mmol) of K_2CO_3, and 0.013 g (0.048 mmol) of 18-crown-6. Yield: 0.210 g (82%). ^{1}H NMR ($CDCl_3$, ppm): 5.23 (OCH_2, s, 4H), 6.88 (CH, d, 2H), 7.10 ($C_{Ar}H$, d, 4H), 7.37 ($C_{Ar}H$, t, 4H), 7.47 ($C_{Ar}H$, q, 4H), 7.63 ($C_{Ar}H$, t, 8H), 7.80 (CH, d, 2H), 7.88

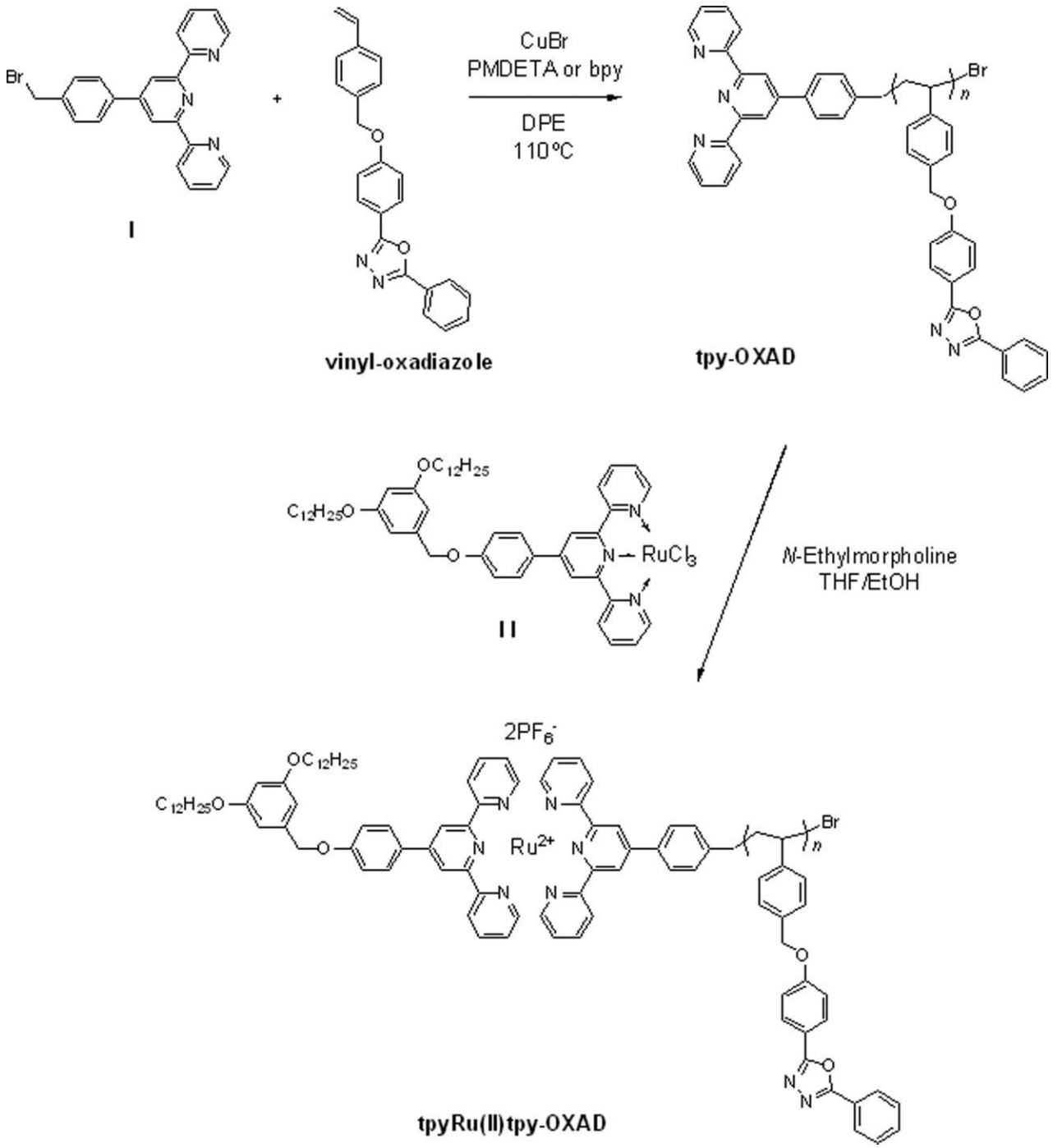

Scheme 2. Preparation of **tpy-OXADs** via ATRP and subsequent complexation toward **tpyRu(II)tpy-OXADs**.

($C_{Ar}H$, td, 4H), 7.96 ($C_{Ar}H$, d, 4H), 8.40 ($C_{Ar}H$, q, 4H), 8.69 ($C_{Ar}H$, d, 4H), 8.75 ($C_{Ar}H$, d, 4H), 8.77 ($C_{Ar}H$, s, 4H). ^{13}C NMR ($CDC1_3$, ppm): 69.79, 115.20, 118.86, 121.40, 123.87, 126.90–128.40, 132.02, 134.11, 136.93, 149.09, 149.82, 155.92, 156.12.

Compound **ditpy-R2**: 0.100 g (0.128 mmol) of **R2**, 0.129 g (0.320 mmol) of **I**, 0.035 g (0.256 mmol) of K_2CO_3, and 0.007 g (0.026 mmol) of 18-crown-6. Yield: 0.145 g (80%). ^1H NMR ($CDCl_3$, ppm): 0.89 (CH_3, t, 6H), 1.24 (CH_2, s, 32H), 1.39 (CH_2, s, 4H), 1.72 (CH_2, m, 4H), 3.96 (OCH_2, t,

4H), 5.22 (OCH_2, s, 4H), 7.05 ($C_{Ar}H$, s, 2H), 7.10 ($C_{Ar}H$, d, 4H), 7.37 ($C_{Ar}H$, t, 4H), 7.62 ($C_{Ar}H$, d, 12H), 7.69 ($C_{Ar}H$, d, 4H), 7.88 ($C_{Ar}H$, td, 4H), 7.96 ($C_{Ar}H$, d, 4H), 8.69 ($C_{Ar}H$, d, 4H), 8.75 ($C_{Ar}H$, d, 4H), 8.77 ($C_{Ar}H$, s, 4H). ^{13}C NMR ($CDC1_3$, ppm): 14.12, 22.72, 26.15, 29.41, 29.63, 31.94, 69.77, 69.79, 115.31, 116.32, 118.91, 121.40, 123.84, 126.28, 127.64, 127.97, 128.18, 129.91, 134.01, 136.87, 138.01, 138.28, 139.30, 149.20, 149.94, 150.50, 156.07, 156.33, 158.34.

Compound **ditpy-R3**: 0.100 g (0.193 mmol) of **R3**, 0.194 g (0.483 mmol) of **I**, 0.053 g (0.386 mmol) of K_2CO_3, and 0.010 g (0.039 mmol) of 18-crown-6. Yield: 0.170 g (76%). ^1H NMR ($CDC1_3$, ppm): 0.77 (CH_2CH_3, m, 10H), 1.08 (CH_2, m, 12H), 2.03 (CH_2, m, 4H), 5.23 (OCH_2, s, 4H), 7.11 ($C_{Ar}H$, d, 4H), 7.37 ($C_{Ar}H$, t, 4H), 7.53 ($C_{Ar}H$, m, 4H), 7.62 ($C_{Ar}H$, m, 8H), 7.73 ($C_{Ar}H$, d, 2H), 7.89 ($C_{Ar}H$, td, 4H), 7.96 ($C_{Ar}H$, d, 4H), 8.69 ($C_{Ar}H$, d, 4H), 8.75 ($C_{Ar}H$, d, 4H), 8.77 ($C_{Ar}H$, s, 4H). ^{13}C NMR ($CDC1_3$, ppm): 13.94, 22.54, 23.78, 29.70, 31.44, 40.48, 55.20, 69.83, 115.29, 118.94, 119.81, 121.10, 121.42, 123.83, 125.60, 127.61, 127.91, 128.23, 134.74, 136.95, 138.04, 138.19, 139.49, 139.64, 149.06, 149.91, 151.60, 155.92, 156.17, 158.17.

Compound **ditpy-R4**: 0.100 g (0.085 mmol) of **R4**, 0.085 g (0.212 mmol) of **I**, 0.023 g (0.169 mmol) of K_2CO_3, and 0.005 g (0.017 mmol) of 18-crown-6. Yield: 0.105 g (68%). ^1H NMR ($CDC1_3$, ppm): 0.78 (CH_2CH_3, m, 30H), 1.11 (CH_2, m, 36H), 2.05 (CH_2, m, 12H), 5.24 (OCH_2,s, 4H), 7.12 ($C_{Ar}H$, d, 4H), 7.37 ($C_{Ar}H$, t, 4H), 7.55 ($C_{Ar}H$, m, 4H), 7.60–7.70 ($C_{Ar}H$, m, 16H), 7.79 ($C_{Ar}H$, q, 6H), 7.90 ($C_{Ar}H$, td, 4H), 7.96 ($C_{Ar}H$, d, 4H), 8.69 ($C_{Ar}H$, d, 4H), 8.75 ($C_{Ar}H$, d, 4H), 8.77 ($C_{Ar}H$, s, 4H). ^{13}C NMR ($CDC1_3$, ppm): 14.01, 22.56, 23.77, 29.68, 31.45, 40.41, 55.25, 69.77, 115.25, 118.87, 119.93, 121.13, 121.41, 123.49, 123.88, 125.64, 126.08, 127.62, 127.94, 128.25, 134.65, 136.95, 137.95, 138.16, 139.59, 139.96, 140.34, 149.11, 151.68, 155.93, 156.17, 158.14.

ATRP of Monomer Vinyl-Oxadiazole Using the Terpyridine Initiator I

A round-bottom flask equipped with a rubber septum, a magnetic stirrer, and a gas inlet/outlet was flamed under vacuum. The initiator **I**, 56.76 mg (0.141 mmol), was added to the flask containing CuBr, 20.25 mg (0.141 mmol), and 2,2′-bipyridine, 44.11 mg (0.282 mmol), or PMDETA, 29.50 μL (0.141 mmol); or CuBr 40.50 mg (0.282 mmol) and PMDETA 50.00 μL (0.282 mmol). These correspond to ratios in mmol, of initiator **I**:CuBr:bpy of 1:1:2 and initiator **I**:CuBr:PMDETA of 1:1:1 or 1:2:2. The system was degassed three times and flushed with argon. The solvent diphenyl ether (2 mL) and different amounts of the monomer **vinyl-oxadiazole** were added to the flask and the mixture was immediately degassed three times and flushed again with argon. The reaction mixture was then immersed in an oil bath and heated at 110 °C for 18 h. After cooling to room temperature $CHCl_3$ (3–4 mL) was added to the reaction mixture to dissolve the polymer. The suspension was filtered for removing most of the catalyst. The polymer was precipitated in a large excess of methanol (20-fold excess by volume). The obtained **tpy–OXAD** was purified by reprecipitation from $CHCl_3$ into ethyl acetate and dried under vacuum (for molecular characteristics see Table 1). ^1H NMR ($CDC1_3$, ppm) for polymer **tpy–OXAD-ii**: 1.4–2.4 (m, 3H oxd polymer and 2H tpy initiator), 5.0 (s, 2H oxd polymer), 6.3–7.6 (m, 9H oxd polymer and 4H tpy initiator), 8.0 (s, 4H oxd polymer and 4H tpy initiator), 8.6 ppm (s, 6H tpy initiator).

General Procedure for the Synthesis of the Semiconducting Dicomplexes ditpyRu(II)tpy-R (R1–R4) and of the Oxadiazole Complexes tpyRu(II)tpy–OXADs

The compounds **ditpy-R1–ditpy-R4** or the polymer **tpy–OXAD-i**, and the didodecyloxy-terpyridine/ruthenium(III) mono-complex **II** were mixed in 25 mL of a 3:1 mixture of THF/EtOH. Five drops of *N*-ethylmorpholine were added and the mixture was heated to reflux for 5 days. After removing insoluble byproducts by filtration through celite, the resulting deep red filtrate was evaporated to almost half of its' volume. Addition of excess of a saturated NH_4PF_6/MeOH solution caused the complex to precipitate as a red powder, which was filtrated and washed with EtOH, H_2O (**ditpyRu(II)tpy-R1-R4** and **tpyRu(II)tpy-OXAD**) and toluene in the case of **ditpyRu(II) tpy-R4** and **tpyRu(II)tpy-OXAD**. The final complex was obtained by reprecipitation from $CHCl_3$ (5 mL) into hexane (50 mL) and dried under vacuum at 40 °C.

Complex **ditpyRu(II)tpy-R1**: 0.040 g (0.038 mmol) of **ditpy-R1**, 0.094 g (0.095 mmol) of **II**. Yield: 80 mg (62%). ^1H NMR (DMSO-d6, ppm): 0.86 (CH_3, s, 12H), 1.11–1.51 (CH_2, m, 72H), 1.72 (CH_2, m, 8H), 4.02 (OCH_2, s, 8H), 5.25 (OCH_2, s, 4H), 5.44 (OCH_2, s, 4H), 6.46 ($C_{Ar}H$, s, 2H), 6.67

Table 1. Reaction Conditions and Molecular Weight Characteristics of the Synthesized **tpy-OXADs**

Polymer[a]	Amine	M_n (^{1}H NMR)	M_n[b]	M_w[b]	M_w/M_n[b]
tpy–OXAD–i[c]	bpy	2785	2080	2825	1.36
tpy–OXAD–ii[c]	bpy	4065	2095	2895	1.38
tpy–OXAD–iii[c]	bpy	2455	2190	2745	1.25
tpy–OXAD–iv[c]	bpy	3820	2815	3700	1.31
tpy–OXAD–v[d]	PMDETA	6960	4765	6300	1.32
tpy–OXAD–vi[d]	PMDETA		5155	6065	1.18
tpy–OXAD–vii[e]	PMDETA		43440	99400	2.29

Reaction conditions:
[a] CuBr, diphenyl ether 10% *w*/*v*, 110 °C.
[b] Molecular weights and polydispersity indices M_w/M_n were determined with size exclusion chromatography ($CHCl_3$, room temperature) using polystyrene standards and UV detection at 254 nm.
[c] Ratio of $[monomer]_0/I/[CuBr]_0/[bpy]_0 = 10/1/1/2$.
[d] Ratio of $[monomer]_0/I/[CuBr]_0/[PMDETA]_0 = 30/1/1/1$.
[e] Ratio of $[monomer]_0/I/[CuBr]_0/[PMDETA]_0 = 30/1/2/2$.

($C_{Ar}H$, s, 4H), 6.91 (CH, d, 2H), 7.15 ($C_{Ar}H$, d, 4H), 7.28 ($C_{Ar}H$, m, 8H), 7.43–7.85 ($C_{Ar}H$, CH, m, 26H), 8.03 ($C_{Ar}H$, m, 8H), 8.38 ($C_{Ar}H$, m, 12H), 9.05 ($C_{Ar}H$, t, 8H), 9.38 ($C_{Ar}H$, d, 8H).

Complex **ditpyRu(II)tpy-R2**: 0.035 g (0.025 mmol) of **ditpy-R2**, 0.061 g (0.061 mmol) of **II**. Yield: 50 mg (54%). ^{1}H NMR (DMSO-d6, ppm): 0.87 (CH_3, s, 18H), 1.11–1.51 (CH_2, m, 108H), 1.72 (CH_2, m, 12H), 4.01 (OCH_2, s, 12H), 5.26 (OCH_2, s, 4H), 5.42 (OCH_2, s, 4H), 6.48 ($C_{Ar}H$, s, 2H), 6.68 ($C_{Ar}H$, s, 4H), 7.20 ($C_{Ar}H$, s, 2H), 7.28 ($C_{Ar}H$, m, 12H), 7.38 ($C_{Ar}H$, d, 4H), 7.53 ($C_{Ar}H$, m, 8H), 7.71 ($C_{Ar}H$, s, 12H), 7.87 ($C_{Ar}H$, d, 4H), 8.04 ($C_{Ar}H$, m, 8H), 8.40 ($C_{Ar}H$, dd, 8H), 9.06 ($C_{Ar}H$, t, 8H), 9.39 ($C_{Ar}H$, d, 8H).

Complex **ditpyRu(II)tpy-R3**: 0.030 g (0.026 mmol) of **ditpy-R3**, 0.064 g (0.065 mmol) of **II**. Yield: 82 mg (90%). ^{1}H NMR (DMSO-d6, ppm): 0.73 (CH_2CH_3, m, 10H), 0.87 (CH_3, m, 12H), 1.08 (CH_2, m, 12H), 1.15–1.51 (CH_2, m, 72H), 1.74 (CH_2, m, 8H), 2.12 (CH_2, m, 4H), 4.01 (OCH_2, t, 8H), 5.23 (OCH_2, s, 4H), 5.42 (OCH_2, s, 4H), 6.48 ($C_{Ar}H$, s, 2H), 6.68 ($C_{Ar}H$, s, 4H), 7.21–7.32 ($C_{Ar}H$, m, 12H), 7.38 ($C_{Ar}H$, d, 4H), 7.52 ($C_{Ar}H$, m, 8H), 7.59–7.77 ($C_{Ar}H$, m, 8H), 7.88 ($C_{Ar}H$, m, 6H), 8.04 ($C_{Ar}H$, m, 8H), 8.42 ($C_{Ar}H$, dd, 8H), 9.06 ($C_{Ar}H$, t, 8H), 9.39 ($C_{Ar}H$, d, 8H).

Complex **ditpyRu(II)tpy-R4**: 0.065 g (0.036 mmol) of **ditpy-R4**, 0.088 g (0.089 mmol) of **II**. Yield: 105 mg (71%). ^{1}H NMR (DMSO-d6, ppm): 0.67–0.92 (CH_2CH_3, m, 42H), 1.08 (CH_2 ,m, 36H), 1.15–1.51 (CH_2, m, 72H), 1.73 (CH_2, m, 8H), 2.13 (CH_2, m, 12H), 4.01 (OCH_2, t, 8H), 5.24 (OCH_2, s, 4H), 5.42 (OCH_2, s, 4H), 6.46 ($C_{Ar}H$, s, 2H), 6.67 ($C_{Ar}H$, s, 4H), 7.21–7.30 ($C_{Ar}H$, m, 12H), 7.34 ($C_{Ar}H$, d, 4H), 7.50 ($C_{Ar}H$, m, 8H), 7.59–7.77 ($C_{Ar}H$, m, 16H), 7.88 ($C_{Ar}H$, m, 12H), 8.02 ($C_{Ar}H$, m, 8H), 8.39 ($C_{Ar}H$, dd, 8H), 9.01 ($C_{Ar}H$, t, 8H), 9.35 ($C_{Ar}H$, d, 8H).

Complex tpyRu(II)tpy-OXAD

0.090 g (0.032 mmol) of **tpy–OXAD-i**, 0.048 g (0.048 mmol) of **II**. Yield: 90 mg (68%). ^{1}H NMR (DMSO-d6, ppm): 0.85 (s, 6H), 1.03–1.49 (m, 36H), 1.50–2.20 (m, 3H oxd polymer and 4H), 4.00 (s, 4H), 5.07 (s, 2H oxd polymer), 5.24 (s, 2H), 6.46 (s, 1H), 6.66 (s, 2H), 6.10–7.65 (m, 9H oxd polymer and 12H), 7.7–8.4 (m, 4H oxd polymer and 8H), 8.98 (s, 4H), 9.29 (s, 4H).

RESULTS AND DISCUSSION

For the preparation of di[didodecyloxy–tpy–Ru(II)-tpy] semiconducting oligomers **ditpyRu(II)tpy–R**, anthracene (**R1**),[44] quinquephenyl (**R2**),[45] fluorene (**R3**),[46] and trifluorene (**R4**)[47] segments were employed, Scheme 1. Starting from the hydroxyl end-functionalized molecules **R1–R4**, their etherification with 4′-(2,2′:6′,2″-terpyridin-4′-yl)benzyl bromide (**I**)[43] afforded the diterpyridine end-functionalized molecules, **ditpy-R1–ditpy-R4**. Subsequent complexation with didodecyloxy–tpy–Ru(III)Cl_3 (**II**)[32] was accomplished using EtOH as the reducing agent and *N*-ethylmorpholine as catalyst for the Ru(III) to Ru(II) reduction. The final semiconducting dicomplexes **ditpyRu(II)tpy–R** (Scheme 1) were isolated from the reaction mixture after counter ion exchange of Cl^- to $PF6^-$ (chloride to hexafluorophosphate) with an addition of excess of methanolic NH_4PF_6

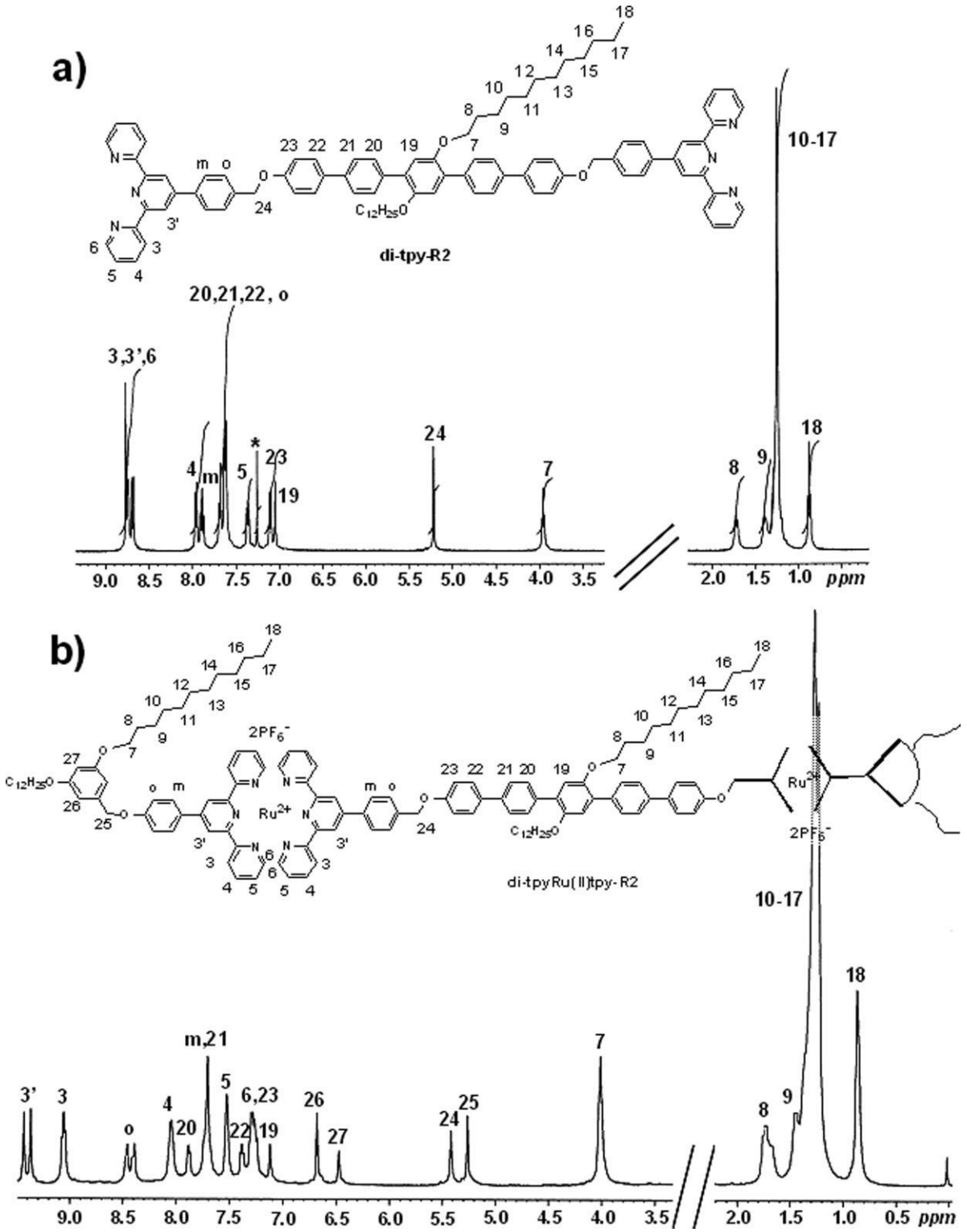

Figure 1. ^{1}H NMR spectra of (a) **ditpy-R2** in $CDCl_3$ at room temperature and (b) of **ditpyRu(II)tpy-R2** in DMSO-d6 at 100 °C.

solution.[48,49] Excess of **II** was effectively removed by redisolving the dicomplexes in $CHCl_3$ and precipitation into *n*-hexane, while for **ditpyRu(II)tpy–R4** washing with toluene can also be performed. These dicomplexes were easily soluble in common organic solvents, including $CHCl_3$,

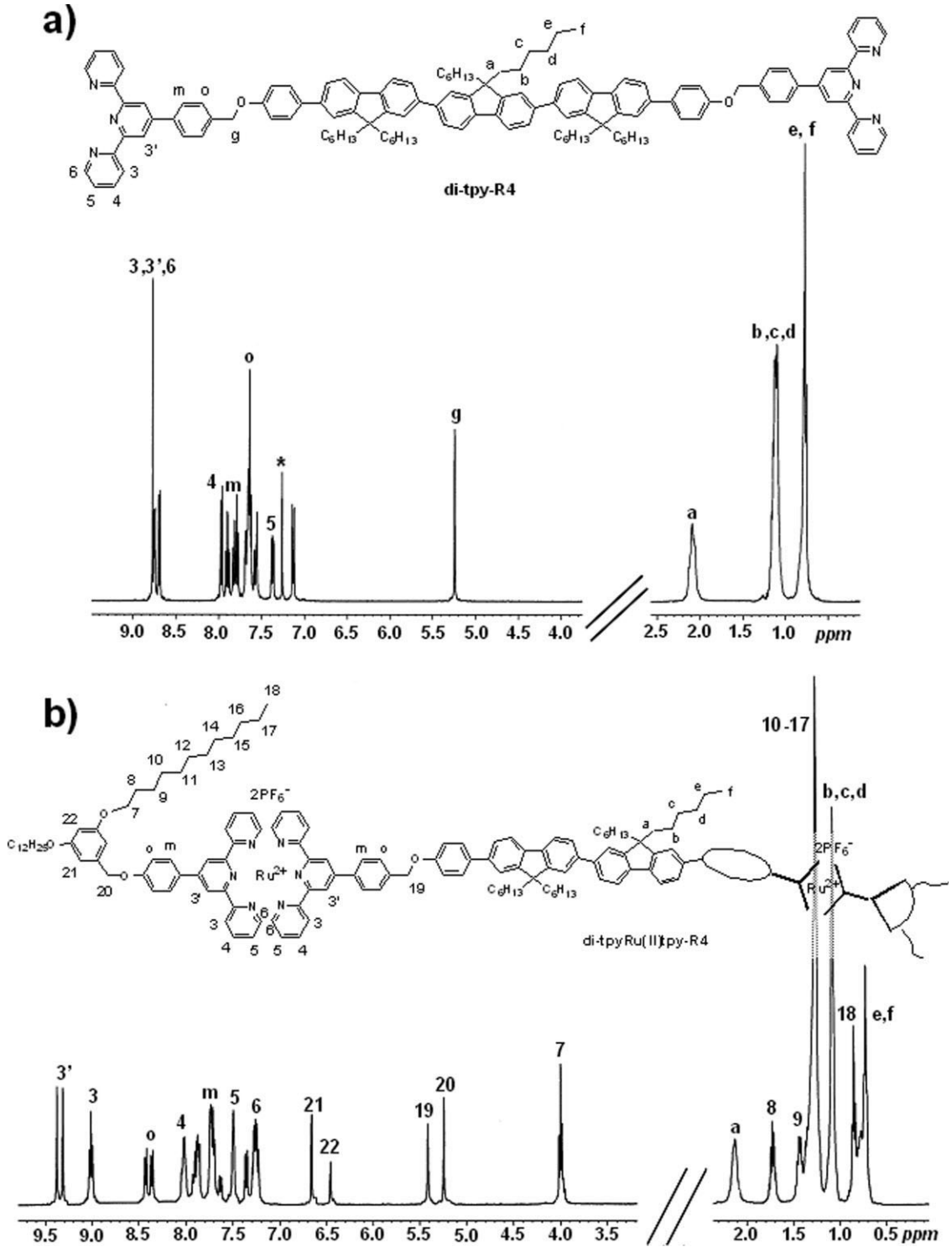

Figure 2. ^{1}H NMR spectra of (a) **ditpy-R4** in $CDCl_3$ at room temperature and (b) of **ditpyRu(II)tpy-R4** in DMSO-d6 at 100 °C.

THF, DMSO, and DMF and were fully characterized using ^{1}H NMR. Representative ^{1}H NMR spectra before and after complexation are given in Figure 1 for **ditpy-R2** and **ditpyRu(II)tpy-R2** and in Figure 2 for **ditpy-R4** and **ditpyRu (II)tpy-R4**. The characteristic downfield shift of

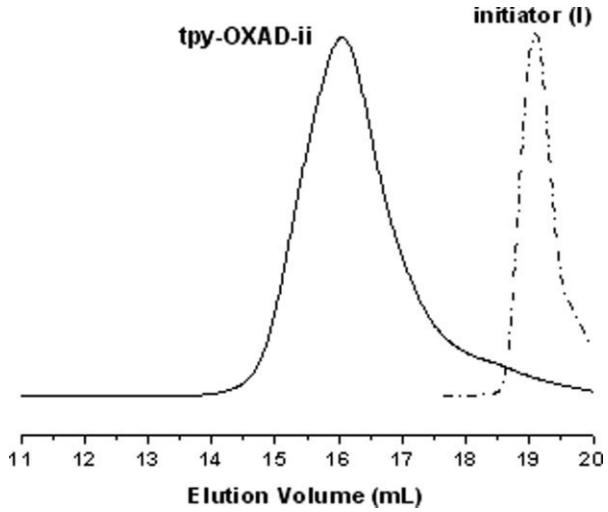

Figure 3. GPC traces of **tpy-OXAD-ii** and of the terpyridine initiator **I** (UV detection at 254 nm).

the 3 and 3′ protons of the tpy moieties after complexation from ~8.7 ppm to ~9 and ~9.35 ppm, respectively, and the upfield shift of the 6 tpy protons from ~8.7 to ~7.3 ppm can be noticed. Additionally, no peaks corresponding to the initial compounds could be found at 8.60–8.80 ppm attributed to the tpy groups of the uncomplexed materials.

Apart from the oligomeric semiconducting dicomplexes, we also prepared semiconducting oxadiazole homopolymers of various molecular weights carrying one didodecyloxy-tpy-Ru(II)-tpy end-group **tpyRu(II)tpy-OXAD** as presented in Scheme 2. 4′-(2,2′:6′,2″-Terpyridin-4′-yl)benzyl bromide (**I**),[43] was used as ATRP mono-functional initiator for the polymerization of monomer **vinyl-oxadiazole**,[44(a),44(b)] producing a series of tpy end-functionalized side chain poly(oxadiazole)s (**tpy-OXAD**, Scheme 2). ATRP polymerizations[36] were carried out using different sets of experimental conditions with respect to base, solvent, and ratios of monomer/initiator/catalyst/base. Polymers of controlled molecular weights and narrow polydispersities were obtained when 2,2′-bipyridine (bpy) or PMDETA (*N,N,N′,N′,N′*-pentamethyldiethylenetriamine) was used as ligands of the Cu(I)/Cu(II) catalyst, but higher M_w copolymers were obtained with PMDETA as the catalyst's ligand, Table 1. More specifically, we found that using a $[monomer]_0/I/[CuBr]_0/[bpy]_0$ ratio of 10/1/1/2 and a $[monomer]_0/I/[CuBr]_0/[PMDETA]_0$ ratio of 30/1/1/1 or 30/1/2/2, at 110 °C in a concentration of 10% *w/v* in diphenyl ether, low-polydispersity polymers with yields in the range of 45–70% were obtained, as shown in Table 1.

It is worth mentioning that due to the use of an uncomplexed-free tpy compound as the ATRP initiator, all crude **tpy–OXADs** prepared were green since the end-tpy functionalities complexated the Cu(II) ions of the catalyst. The crude polymers were uncomplexated from the Cu(II) ions by redissolving them in DMF and addition of concentrated HCl. The desired **tpy–OXADs** were obtained as white powder-like materials after treatment with aqueous Na_2CO_3 in DMF.[50] This means that simultaneously with the catalytic system employed for the ATRP (CuBr/bpy or CuBr/PMDETA), a second catalytic system such as CuBr/tpy was formed *in situ*, which is much weaker than the first one. ATRP reactions using uncomplexed, free tpy units are usually known to be unsuccessful possibly due to the reduced solubility of the tpy–Cu(II) complexes leading to inadequate deactivation rates,[51] although some successful cases have been reported.[32]

All synthesized polymers exhibited good solubilities in a wide range of organic solvents, including $CHCl_3$, THF, and DMF enabling their characterization with GPC and ^1H NMR techniques. Any unreacted oxadiazole monomer was

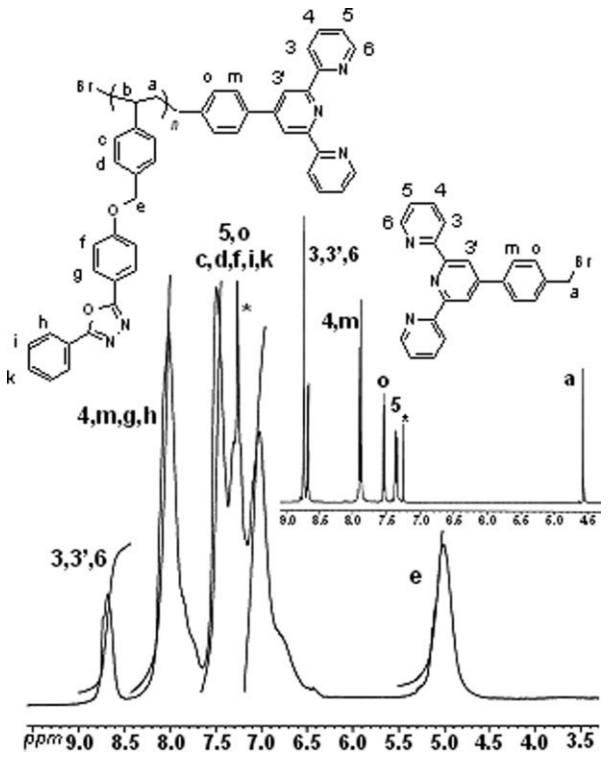

Figure 4. ^1H NMR spectrum in $CDCl_3$ at room temperature of **tpy-OXAD-ii**. The inset shows the ^1H NMR spectrum of the terpyridine initiator **I** in $CDCl_3$ at room temperature.

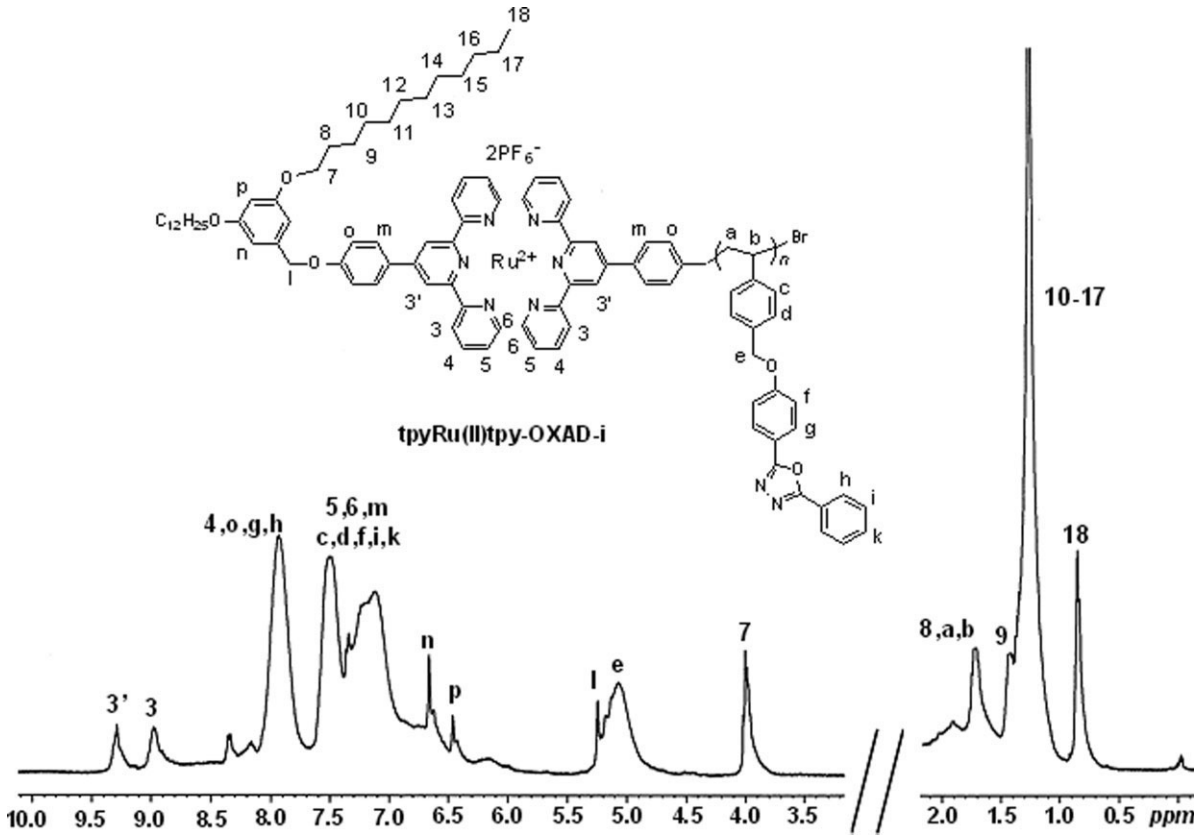

Figure 5. ^{1}H NMR spectrum in DMSO-d6 at 100 °C of the polymeric monocomplex **tpyRu(II)tpy-OXAD-i**.

effectively removed using dissolution of the reaction mixture and precipitation in ethyl acetate which is a selective solvent for the **vinyl-oxadiazole** monomer. GPC was used to make sure that no trace of unreacted initiator remained in the polymers and to examine the effectiveness of the synthetic process in obtaining polymers with narrow polydispersities. Indeed, GPC did not reveal any initiator **I** residual, as shown, for example, in Figure 3 for **tpy–OXAD-ii**. The molecular weights of **tpy–OXADs** vary between 2000 and 43,000 and the polydispersity indices (M_w/M_n) for the low-molecular-weight ones, entries **i–vi** of Table 1, are in the range of 1.18–1.38.

Since the molecular weight values obtained from GPC are based on calibration with polystyrene standards and also since terpyridines are known to interact with the stationary phase of the GPC columns resulting in apparent lower molar mass values,[25a] we additionally used the ^{1}H NMR end-group analyses technique to estimate the true M_n values of our polymers. A representative ^{1}H NMR spectrum of polymer **tpy–OXAD-i** with the assignment of all peaks is depicted in Figure 4. Molecular weight calculations were based on the 3′, 3, and 6 aromatic protons of the terpyridine initiator **I** at 8.69–8.77 ppm and the signal at 5.0 ppm corresponding to the methylene protons in the α-position to the oxygen of the monomer **vinyl-oxadiazole**. The end-group analyses results are given in Table 1 and, indeed, they deviate from the respective GPC M_n results. The incorporation of initiator **I** onto the polymeric chains of **tpy–OXAD** and the initiation efficiency were also confirmed by ^{1}H NMR spectroscopy. As shown in Figure 4 for the polymer **tpy–OXAD-i**, the signal at 4.6 ppm, which is assigned to the terminal protons next to the halogen atoms of the initiator, has totally disappeared after the polymerization while the typical signals of the 3′, 3, and 6 aromatic protons of the terpyridine initiator **I** centered at 8.7 ppm are present, showing the effectiveness of the synthetic process.

Complexation of the free end-tpy moiety of **tpy–OXAD** with didodecyloxy-tpy-Ru(III)Cl_3 (**II**)

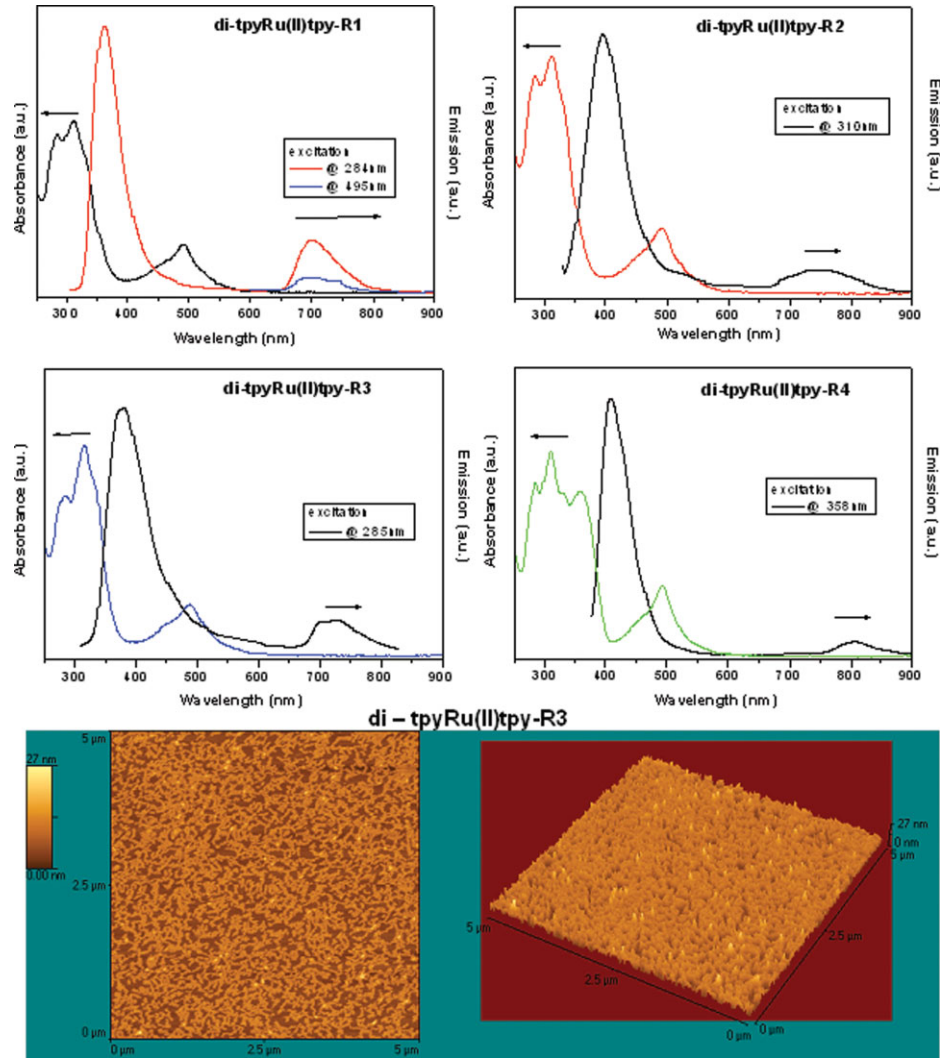

Figure 6. Absorbance and photoluminescence spectra of dendronized **ditpyRu (II)tpy-R** semiconducting oligomeric dicomplexes in $CHCl_3$ solutions 10^{-6} M; and AFM image (phase and topographical three-dimensional images at 5 × 5 μm tapping mode) of **ditpyRu(II)tpy-R3** spin coated on mica from a $\sim 10^{-6}$ M $CHCl_3$ solution.

was performed under standard complexation conditions, affording the final polymeric complex **tpyRu(II)tpy-OXAD** (Scheme 2) whose structural perfection was also proven by ^{1}H NMR, Figure 5 for **tpyRu(II)tpy-OXAD-i**.

For all the tpy–Ru(II)–tpy end-capped semiconducting oligomers and polymers, their UV-Vis spectroscopic characterization in dilute $CHCl_3$ solutions showed typical MLCT (metal-to-ligand charge transfer) absorptions of the tpy–Ru(II)–tpy moieties at ~495 nm as well as the π–π^* transitions of the terpyridine ligands at ~310 nm, with no band at 414 nm due to residues of $Ru(III)Cl_3$ monocomplex, Figure 6. The di(styryl)-anthracene dicomplex **ditpyRu(II)tpy-R1** exhibited one

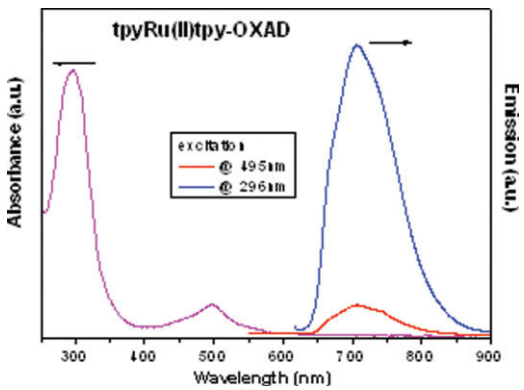

Figure 7. Absorbance and photoluminescence spectra of **tpyRu(II)tpy-OXAD** in $CHCl_3$ solution of 10^{-6} M concentration.

additional absorption band at 414 nm, which overlapped with the strong absorption at 496 nm, Figure 6(a). The fluorene **ditpyRu(II)tpy-R3** and trifluorene **ditpyRu(II)tpy-R4** dicomplexes exhibited additional absorptions at 326 and 360 nm, respectively, Figure 6(c,d). Even for the single tpy–Ru(II)–tpy-bearing oxadiazole polymeric complex **tpyRu(II)tpy-OXAD**, the MLCT absorption band at 497 nm was easily detected, Figure 7, whereas side-chain oxadiazole homopolymers are known to exhibit only one absorption band at 294 nm.

The photoluminescence properties of the semiconducting tpy–Ru(II)–tpy complexes were examined after excitation either at the absorption maxima of the organic part or at the MLCT absorption band of the tpy–Ru(II)–tpy units, Figures 6 and 7. In the second case, weaker emissions at the red spectrum region were detected (700–800 nm) whereas, in the first case, intense emissions from the semiconducting segments and from the tpy–Ru(II)–tpy segments were observed. An unexpected behavior was observed for the **tpyRu(II)tpy–OXAD** monocomplex, Figure 7, with a strong red light emission centered at 706 nm after excitation at 296 nm, which was orders of magnitudes stronger than the one after excitation at the MLCT maxima (495 nm), but in no case was the typical blue emission of side polyoxadiazoles detected at $\sim$360 nm.

As aforementioned, the presence of alkoxy tails may possibly impose an organization ability onto the final metallo-semiconducting material. Indeed, AFM examination of the **ditpyRu(II)tpy-R3** dicomplex, shown in Figure 6, after spin coating of a dilute $CHCl_3$ solution on freshly cleaved mica, revealed a fine and continuous "string-like" structure at the nanometer scale. A possible explanation can be a phase separation of the metal ions from the fully organic segments and also the high affinity of the long aliphatic chains at the very ends of these molecules. A more in-depth evaluation of their organizational behavior is in progress to understand the driving forces governing their self-assembly and the arrangement of the chromophoric parts in the solid state.

CONCLUSIONS

Since the terpyridine (tpy) functionalities are ideal candidates for the development of supramolecular entities due to their selective metal/ligand coordination chemistry, we prepared ditpy end-functionalized semiconducting compounds and mono-tpy end-functionalized side-chain poly(oxadiazole)s that were used as building blocks for the attachment of prefabricated didodecyloxy–tpy–$Ru(III)Cl_3$ entities. All metal-bearing oligomers and polymers presented enhanced solubilities in common organic solvents, and their structural and optoelectronic characteristics were thoroughly investigated. The combination of these fully organic semiconducting oligomeric and polymeric compounds with tpy–metal ion complexes opens new ways for the construction of new supramolecular materials with predetermined optical properties.

The authors thank Dr. Vlassoula Bekiari, University of Patras, for helpful discussions. This work was supported, in part, by the Greek Ministry of Development under the research grant PENED 03ED118 "Organic Solar Cells," cofinanced by the E.U.-European Social Fund (75%) and the Greek Ministry of Development-GSRT (25%).

REFERENCES AND NOTES

1. (a) Balzani, V.; Juris, A.; Venturi, M.; Campagna, S.; Serroni, S. Chem Rev 1996, 96, 759–833; (b) Gorman, C. Adv Mater 1998, 10, 295–309; (c) Constable, E. C. Chem Commun 1997, 1073–1080; (d) Van Manen, H.-J.; Van Veggel, F. C. J. M.; Reihnbout, D. N. Top Curr Chem 2001, 217, 121–162; (e) Archut, A.; Vögtle, F. Chem Soc Rev 1998, 27, 233–240; (f) Schubert, U. S.; Eschbaumer, C. Angew Chem Int Ed Engl 2002, 41, 2892–2926; (g) Gohy, J.-F.; Lohmeijer, B. G. G.; Schubert, U. S. Chem Eur J 2003, 9, 3472–3479.
2. Kalyanasundaram, K. Coord Chem Rev 1982, 46, 159–244.
3. (a) Buda, M.; Kalyuzhny, G.; Bard, A. J. J Am Chem Soc 2002, 124, 6090–6098; (b) Slinker, J. D.; Defranco, J. A.; Jaquith, M. J.; Silveira, W. R.; Zhong, Y.-W.; Moran-Mirabal, J. M.; Craighead, H. G.; Abruna, H. D.; Marohn, J. A.; Malliaras, G. G. Nature Mater 2007, 6, 897–899.
4. (a) Farah, A. A.; Pietro, W. J. Polym Bull 1999, 43, 135–142; (b). Marin, V.; Holder, E.; Hoogenboom, R.; Schubert, U. S. Chem Soc Rev 2007, 36, 618–635.
5. Balzani, V.; Juris, A. Coord Chem Rev 2001, 211, 97–115.
6. (a) Bard, A. J.; Gao, F. G. J Am Chem Soc 2000, 122, 7426–7427; (b) Holder, E.; Langeveld, B. M. W.; Schubert, U. S. Adv Mater 2005, 17, 1109–1121.
7. (a) Juris, A.; Balzani, V.; Barigelletti, F.; Campagna, S.; Belser, P.; Von Zelewsky, A. Coord Chem

Rev 1988, 84, 85–277; (b) Medlycott, E. A.; Hanan, G. S. Coord Chem Rev 2006, 250, 1763–1782.
8. Baranoff, E.; Collin, J.-P.; Flamigni, L.; Sauvage, J.-P. Chem Soc Rev 2004, 33, 147–155.
9. (a) Smith, A. P.; Fraser, C. L. Macromolecules 2003, 36, 2654–2660; (b) Smith, A. P.; Fraser, C. L. J Polym Sci Part A: Polym Chem 2002, 40, 4250–4255.
10. Kalyanasundaram, K. Photochemistry of Polypyridine and Porphyrin Complexes, 1st ed.; Academic Press: San Diego, 1992.
11. Roundhill, D. M. Photochemistry and Photophysics of Metal Complexes; Plenum Press: New York, 1994.
12. McCusker, J. K. Acc Chem Res 2003, 36, 876–887.
13. Sauvage, J. P.; Collin, J. P.; Chambron, J. C.; Guillerez, S.; Coudret C.; Balzani, V.; Barigelletti, F.; De Cola, L.; Flamigni, L. Chem Rev 1994, 94, 993–1019.
14. Morgan, G. T.; Burstall, F. H. J Chem Soc 1932, 20–30.
15. Thompson, A. M. W. C. Coord Chem Rev 1997, 160, 1–52.
16. Jameson, D. L.; Guise, L. E. Tetrahedron Lett 1991, 32, 1999–2002.
17. Cooke, M. W.; Wang, J.; Theobald, I.; Hanan, G. S. Synth Commun 2006, 36, 1721–1726.
18. Kröhnke, F. Synthesis 1976, 1–24.
19. (a) Constable, E. C. Chem Soc Rev 2007, 36, 246–253; (b) Heller, M.; Schubert, U. S. Eur J Org Chem 2003, 947–961.
20. Vaduvescu, S.; Potvin, P. G. Eur J Inorg Chem 2004, 1763–1769.
21. Barigelletti, F.; Flamigni, L.; Balzani, V.; Collin, J.-P.; Sauvage, J.-P.; Sour, A. New J Chem 1995, 19, 793–798.
22. Medlycott, E. A.; Hanan, G. S. Chem Soc Rev 2005, 34, 133–142.
23. (a) Kelch, S.; Rehahn, M. Macromolecules 1999, 32, 5818–5828; (b) Knapp, R.; Kelch, S.; Schmelz, O.; Rehahn, M. Macromol Symp 2003, 204, 267–286.
24. (a) Shunmugam, R.; Tew, G. N. J Am Chem Soc 2005, 127, 13567–13572; (b) Aamer, K. A.; Tew, G. N. Macromolecules 2004, 37, 1990–1993; (c) Tew, G. N.; Aamer, K. A.; Shunmugan, R. Polymer 2005, 46, 8440–8447.
25. (a) El-ghayoury, A.; Hofmeiier, H.; Ruiter, B.; Schubert, U. S. Macromolecules 2003, 36, 3955–3959; (b) Wong, C. T.; Chan, W. K. Adv Mater 1999, 11, 455–459.
26. Zhou, G.; Harruna, I. I. Macromolecules 2005, 38, 4114–4123.
27. Guerrero-Sanchez, C.; Lohmeijer, B. G. G.; Meier, M. A. R.; Schubert, U. S. Macromolecules 2005, 38, 10388–10396.
28. (a) Lohmeijer, B. G. G.; Schubert, U. S. Angew Chem Int Ed 2002, 41, 3825–3829; (b) Meier, M. A. R.; Wouters, D.; Ott, C.; Guillet, P.; Fustin, C.-A.; Gohy, J.-F.; Schubert, U. S. Macromolecules 2006, 39, 1569–1576; (c) Hofmeier, H.; Hoogenboom, R.; Wouters, M. E. L.; Schubert, U. S. J Am Chem Soc 2005, 127, 2913–2921; (d) Duprez, V.; Biancardo, M.; Spanggaard, H.; Krebs, F. Macromolecules 2005, 38, 10436–10448; (e) Kimura, M.; Iwashima, Y.; Ohta, K.; Hanabusa, K.; Shirai, H. Macromolecules 2005, 38, 5055–5059.
29. Heller, M.; Schubert, U. S. Macromol Rapid Commun 2001, 22, 1358–1363.
30. Aamer, K. A.; Shunmugan, R.; Tew, G. In Block Copolymers in Nanoscience; Lazzari, M.; Liu, G.; Lecommandoux, S., Eds.; Wiley-VCH: Weinheim, 2006; Chapter 8, pp 169–189.
31. (a) Newkome, G. R.; He, E.; Moorefield, C. N. Chem Rev 1999, 99, 1689–1746; (b) Newkome, G. R.; He, E. J Mater Chem 1997, 7, 1237–1244; (c) Newkome, G. R.; He, E. Macromolecules 1998, 31, 4382–4386.
32. Tzanetos, N.; Andreopoulou, A. K.; Kallitsis, J. K. J Polym Sci Part A: Polym Chem 2005, 43, 4838–4848.
33. Andreopoulou, A. K.; Kallitsis, J. K. Eur J Org Chem 2005, 4448–4458.
34. (a) Newkome, G. R.; Cho, T. J.; Moorefield, C. N.; Baker, G. R.; Saunders, M. J.; Cush, R.; Russo, P. S. Angew Chem Int Ed 1999, 38, 3717–3721; (b) Newkome, G. R.; Cho, T. J.; Moorefield, C. N.; Cush, R.; Russo, P. S.; Godinez, L. A.; Saunders, M. J.; Mohapatra, P. Chem Eur J 2002, 8, 2946–2954.
35. (a) El-ghayoury, A.; Schenning, A. P. H. J.; van Hal, P. A.; Weidl, C. H.; van Dongen, J. L. J.; Janssen, R. A. J.; Schubert, U. S.; Meijer, E. W. Thin Solid Films 2002, 403, 97–101; (b) Khatyr, A.; Ziessel, R. J Org Chem 2000, 65, 3126–3134.
36. (a) Coessens, V.; Pintauer, T.; Matyjaszewski, K. Prog Polym Sci 2001, 26, 337–377; (b) Xia, J.; Matyjaszewski, K. Chem Rev 2001, 101, 2921–2990; (c) Kamigaito, M.; Ando, T.; Sawamoto, M. Chem Rev 2001, 101, 3689–3746.
37. (a) Schluter, A. D. Top Curr Chem 2005, 245, 151–191; (b) Andreopoulou, A. K.; Carbonnier, B.; Kallitsis, J. K.; Pakula, T. Macromolecules 2004, 37, 3576–3587; (c) Riala, P.; Andreopoulou, A.; Kallitsis, J.; Gitsas, A.; Floudas, G. Polymer 2006, 47, 7241–7250; (d) Aamer, K. A.; Tew G. N. Macromolecules 2007, 40, 2737–2744; (e) Aamer, K. A.; de Jeu, W. H.; Tew G. N. Macromolecules 2008, 41, 2022–2029.
38. (a) Percec, V.; Ahn, C.-H.; Barboiu, B. J Am Chem Soc 1997, 119, 12978–12979; (b) Percec, V.; Ahn, C. H.; Ungar, G.; Yeardley, D. J. P.; Möller, M.; Sheiko, S. S. Nature (London) 1998, 391, 161–164; (c) Percec, V.; Ahn, C.-H.; Cho, W.-D.;

Jamieson, A. M.; Kim, J.; Leman, T.; Schmidt, M.; Gerle, M.; Möller, M.; Prokhorova, S. A.; Sheiko, S. S.; Cheng, S. Z. D.; Zhang, A.; Ungar, G.; Yearley, D. J. P. J Am Chem Soc 1998, 120, 8619–8631; (d) Percec, V.; Cho, W.-D.; Ungar, G.; Yeardley, D. J. P. Angew Chem Int Ed 2000, 39, 1597–1602; (e) Percec, V.; Cho, W. D.; Ungar, G.; Yeardley, D. J. P. J Am Chem Soc 2001, 123, 1302–1315; (f) Percec, V.; Glodde, M.; Bera, T. K.; Miura, Y.; Shiyanovskaya, I.; Singer, K. D.; Balagurusamy, V. S. K.; Heiney, P. A.; Schnell, I.; Rapp, A.; Spiess, H.-W.; Hudson, S. D.; Duan, H. Nature 2002, 419, 384–387; (g) Percec, V.; Won, B. C.; Peterca, M.; Heiney, P. A. J Am Chem Soc 2007, 129, 11265–11278; (h) Percec, V.; Rudick, J. G.; Peterca, M.; Heiney, P. A. J Am Chem Soc 2008, 130, 7503–7508; (i) Rudick, J. G.; Percec, V. Acc Chem Res 2008, 41, 1641–1652.

39. (a) Zubarev, E. R.; Stupp, S. I. J Am Chem Soc 2002, 124, 5762–5773; (b) Messmore, B. W.; Hulvat, J. F.; Sone, E. D.; Stupp, S. I. J Am Chem Soc 2004, 126, 14452–14458; (c) Harrington, D. A.; Behanna, H. A.; Tew, G. N.; Claussen, R. C.; Stupp, S. I. Chem Biol 2005, 12, 1085–1091; (d) Zubarev, E. R.; Sone, E. D.; Stupp, S. I. Chem Eur J 2006, 12, 7313–7327; (e) Palmer, L. C.; Velichko, Y. S.; Olvera De La Cruz, M.; Stupp, S. I. Phil Trans R Soc A 2007, 365, 1417–1433; (f) Palmer, L. C.; Stupp, S. I. Acc Chem Res 2008, 41, 1674–1684.
40. (a) Kim, H.-J.; Zin, W.-C.; Lee, M. J Am Chem Soc 2004, 126, 7009–7014; (b) Bae, J.; Choi, J.-H.; Yoo, Y.-S.; Oh, N.-K.; Kim, B.-S.; Lee, M. J Am Chem Soc 2005, 127, 9668–9669; (c) Genson, K. L.; Holzmueller, J.; Ornatska, M.; Yoo, Y.-S.; Par, M.-H.; Lee, M.; Tsukruk, V. V. Nano Lett 2006, 6, 435–440; (d) Hong, D.-J.; Lee, E.; Lee, J.-K.; Zin, W.-C.; Han, M.; Sim, E.; Lee, M. J Am Chem Soc 2008, 130, 14448–14449; (e) Ryu, J.-H.; Tang, L.; Lee, E.; Kim, H.-J.; Lee, M. Chem Eur J 2008, 14, 871–881; (f) Lee, E.; Huang, Z.; Ryu, J.-H.; Lee, M. Chem Eur J 2008, 14, 6957–6966; (g) Kim, H.-J.; Lim, Y.-B.; Lee, M. J Polym Sci Part A: Polym Chem 2008, 46, 1925–1935.
41. (a) Fréchet, J. M. J.; Gitsov, I.; Monteil, T.; Rochat, S.; Sassi, J.-F.; Vergelati, C.; Yu, D. Chem Mater 1999, 11, 1267–1274; (b) Gitsov, I.; Lambrych, K. R.; Remnant, V. A.; Pracitto, R. J Polym Sci Part A: Polym Chem 2000, 38, 2711–2727; (c) Gitsov, I. J Polym Sci Part A: Polym Chem 2008, 46, 5295–5314.
42. (a) Jonkheijm, P.; van der Shoot, P.; Schenning, A. P. H. J.; Meijer, E. W. Science 2006, 313, 80–83; (b) Hoeben, F. J. M.; Jonkheijm, P.; Meijer, E. W.; Schenning, A. P. H. J Chem Rev 2005, 105, 1491–1546; (c) Jonkheijm, P.; Hoeben, F. J. M.; Kleppinger, R.; van Herrikhuyzen, J.; Schenning, A. P. H. J.; Meijer, E. W. J Am Chem Soc 2003, 125, 15941–15949; (d) Wu, J.; Pisula, W.; Müllen, K. Chem Rev 2007, 107, 718–747; (e) Ajayaghosh, A.; Praveen, V. K. Acc Chem Res 2007, 40, 644–656.
43. Hanabusa, K.; Nakamura, A.; Koyama, T.; Shirai, H. Makromol Chem 1992, 193, 1309–1319.
44. (a) Tzanetos, N. P.; Kallitsis, J. K. J Polym Sci Part A: Polym Chem 2005, 43, 1049–1061; (b) Tzanetos, N. P.; Kallitsis, J. K. Chem Mater 2004, 16, 2648–2655; (c) Konstandakopoulou, F. D.; Kallitsis, J. K. J Polym Sci Part A: Polym Chem 1999, 37, 3826–3937.
45. Kakali, F.; Kallitsis, J.; Pakula, T.; Wegner, G. Macromolecules 1998, 31, 6190–6198.
46. Chochos, C. L.; Govaris, G. K.; Kakali, F.; Yiannoulis, P.; Kallitsis, J. K.; Gregoriou, V. G. Polymer 2005, 46, 4654–4663.
47. (a) Tsolakis, P. K.; Kallitsis, J. K. Chem Eur J 2003, 9, 936–943; (b) Chochos, C. L.; Papakonstandopoulou, D.; Economopoulos, S. P.; Gregoriou, V. G.; Kallitsis, J. K. J Macromol Sci Part A 2006, 43, 419–431.
48. Potts, K. T.; Usifer, D. A.; Guadlup, A.; Abruna, H. D. J Am Chem Soc 1987, 109, 3961–3967.
49. Constable, E. C.; Cargill Thomson, A. M. W.; Tocher, D. A.; Daniels, M. A. M. New J Chem 1992, 16, 855–867.
50. Potts, K. T.; Usifer, D. A. Macromolecules 1988, 21, 1985–1991.
51. Kickelbick, G.; Matyjaszewski, K. Macromol Rapid Commun 1999, 20, 341–346.